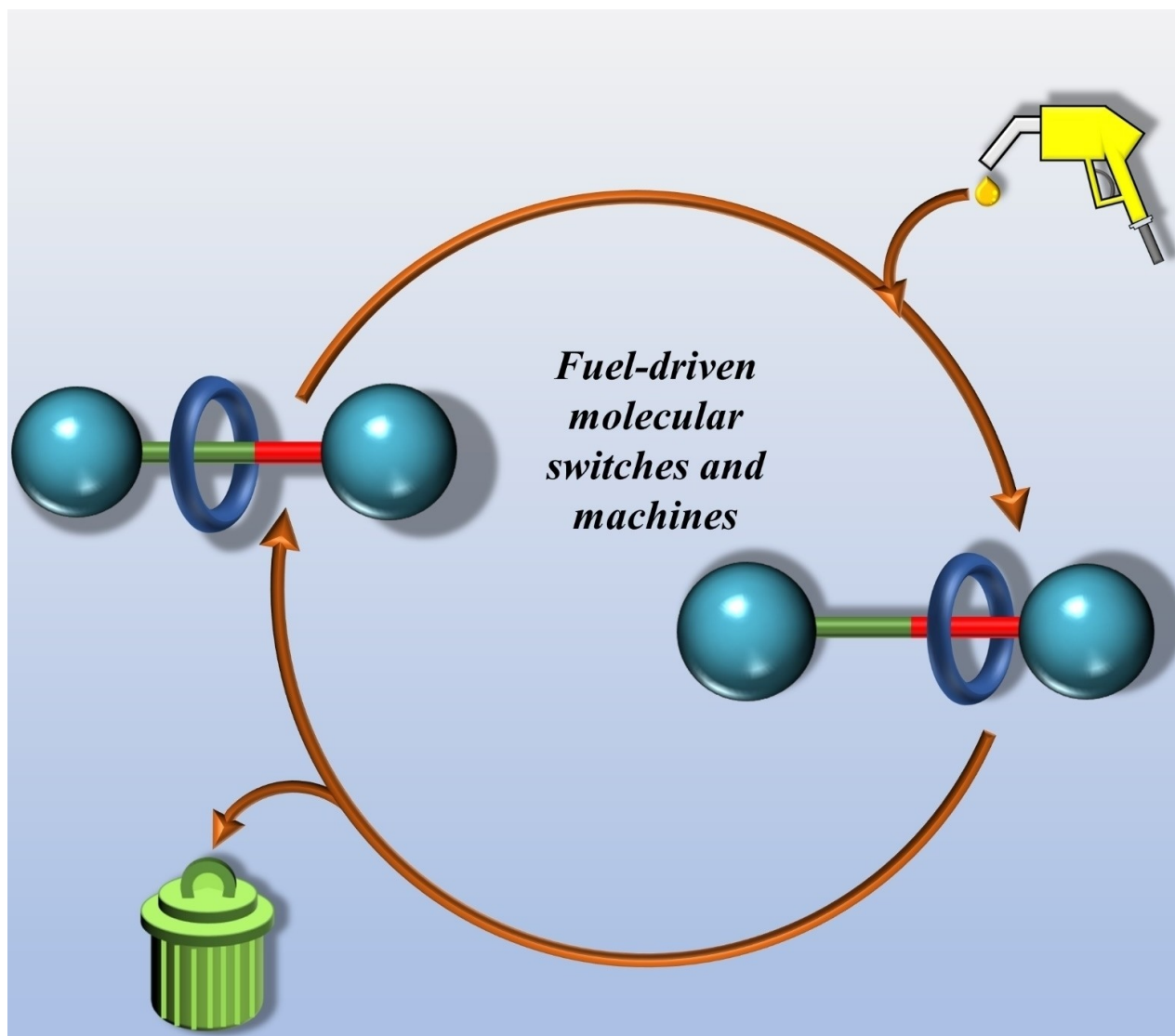


Recent Advances in Fuel-Driven Molecular Switches and Machines

Renitta Benny⁺, Diptiprava Sahoo⁺, Ajith George, and Soumen De^{*[a]}



The molecular switches and machines arena has entered a new phase in which molecular machines operate under out-of-equilibrium conditions using appropriate fuel. Unlike the equilibrium version, the dissipative off-equilibrium machines necessitate only one stimulus input to complete each cycle and decrease chemical waste. Such a *modus operandi* would set

significant steps towards mimicking the natural machines and may offer a platform for advancing new applications by providing temporal control. This review summarises the recent progress and blueprint of autonomous fuel-driven off-equilibrium molecular switches and machines.

1. Introduction

Chemists have always taken inspiration from Nature and aspire not only to mimic those functions but also to achieve beyond what Nature can offer. The field of molecular machines^[1] is no exception. Very recently, with the rise of dissipative off-equilibrium supramolecular architectures,^[3] the field of molecular switches and machines is shifting its gear towards dissipative off-equilibrium switches and machines.^[4] To date, various types of synthetic molecular machines are reported, such as pumps,^[5] muscles,^[6] walkers,^[7] switchable catalysts^[8] and others; most of them are non-autonomous and operate under equilibrium conditions.^[9] This is not surprising, as stable switches and machines are generally easy to work with, characterise and store. Typically, sequential addition of more than one stimuli to complete each operating cycle is needed.^[10] In contrast, many biotic machines work autonomously by hydrolysing high-energy chemical fuels such as ATP and GTP.^[11]

Suppose an artificial molecular machine performs a similar task as bio-molecular machines do. In that case, the synthetic machines must undergo autonomous unidirectional motion by dissipating energy from a continuous external source. These characteristics of autonomy and energy dissipation are directly correlated with the ability of a device to function away from thermal equilibrium. This criterion is intrinsic to living systems but epitomises an arduous task for synthetic systems.

These dissipative machines have vastly different properties than their equilibrium analogues. As the off-equilibrium switches and machines require only one stimulus input to complete each cycle, the system will operate autonomously and decrease chemical waste. Equilibrium molecular switches and machines' properties are time-independent, whereas the characteristics of out-of-equilibrium molecular switches and machines change with time. Such a change in *modus operandi* would set significant steps towards mimicking the natural machines. Moreover, the dissipative off-equilibrium molecular machines may deliver a platform for advancing new applications by providing temporal control.

Therefore, the field of dissipative off-equilibrium molecular switches and machines has recently gained enormous interest.^[12] It is easily visible that the number of publications on dissipative off-equilibrium molecular switches and machines is exponentially increasing each year. This review will summarise the progress and blueprint of autonomous fuel-driven off-equilibrium molecular switches and machines. It will be structured according to the nature of the respective stimuli. The review will not cover fuel-driven out-of-equilibrium self-assembly, and the readers are suggested to take a look at other excellent reviews on this topic.^[3]

2. Terminology

The following section will briefly discuss several terminologies in the field as terminology needs to be used reliably to convey scientific thoughts successfully. According to the Cambridge Dictionary, a machine is "a piece of equipment with several moving parts that uses power to do a particular type of work". In 2007, David Leigh proposed a formal definition of some standard terms such as "machine", "switch", "motor", and others.^[13] Molecular "machines" are those molecules or supramolecular systems that undergo mechanical movements such as translations, rotations, conformational or configurational movements—that is, a net nuclear movement in the molecular world—upon application of an appropriate stimulus and cause something to be accomplished. While motors^[2] represent the more refined and intricate version of machines with net directionality, molecular switches are a more straightforward version of the molecular machine without any directionality. Thus, motors can perform external work, while switches do not.

A stimulus is a reagent or a system of reagents (chemical or light) that causes the mechanical movement in machines. The term "fuel" is also a kind of stimulus capable of performing a complete cycle of motion of molecular machines. According to these definitions, light will always be both stimulus and fuel if the backward process occurs in the dark or with the same wavelength of light. Generally, fuel is a reagent that feeds a molecular motor to perform oriented motions, generating waste at the same time. In the next section, we will be describing the terminology related to equilibria, such as far-from-equilibrium, non-equilibrium, off-equilibrium, out-of-equilibrium, away-from-equilibrium and dissipative states.

[a] R. Benny,* D. Sahoo,* A. George, Prof. Dr. S. De
School of Chemistry
Indian Institute of Science Education and Research Thiruvananthapuram
(IISER-TVM)
Thiruvananthapuram 695551 (India)
E-mail: soumende@iisertvm.ac.in

[*] These authors contributed equally to this work.

 © 2022 The Authors. Published by Wiley-VCH GmbH. This is an open access article under the terms of the Creative Commons Attribution Non-Commercial License, which permits use, distribution and reproduction in any medium, provided the original work is properly cited and is not used for commercial purposes.

3. Design Principle

Before discussing the specific examples, this section will briefly describe the thermodynamic background of the out-of-equilibrium system. To understand out-of-equilibrium states, the diverse regions of an idealised potential energy diagram that outlines the thermodynamic characteristics of a chemical system will be discussed. A system existing in a global minimum on the potential energy surface represents the thermodynamic equilibrium state. It may be dynamic if the energy barriers for interconversion between states are sufficiently low. Once a system reaches equilibrium, it can sustain its equilibrium state without the supply of any external energy, and the system is stable over time. The system's composition can be determined by the relative thermodynamic stabilities of different states.

However, the relative thermodynamic stabilities of various states do not dictate the system's composition when the system is not at equilibrium. The system's composition is determined by the available external energy and barrier height to convert other states. Accordingly, a local minimum can be populated over the global minimum in the presence of external energy input.

Various off-equilibrium states may arise depending on the local minimum's activation barrier to reach other states. Suppose the activation barrier is higher than the available thermal energy ($E_a \geq RT$). In that case, the system cannot evolve to another state as it has insufficient energy to escape from the

energy well and is called kinetically trapped (KT). This type of off-equilibrium state is stable over time, and no energy is required to sustain the KT state. However, suppose the activation barrier is lower or similar to available thermal energy ($E_a \leq RT$). In that case, the out-of-equilibrium state evolves to a more stable one within the timescale of the experiment. It is then called to be in a metastable state (MS). So, the difference between a KT and an MS behaviour is the timescale and not absolute.

Another off-equilibrium other than the KT and MS state is possible. This type of system is not stable on the experimental timescale and can only be observed in the presence of an external energy source. As soon as the energy source is removed, the off-equilibrium state vanishes into an available minimum (either local or global). This high-energy, barrier-less state is called a dissipative (D) state, as this state only exists by dissipating the available energy to the surroundings. Thus, the system may achieve a stationary off-equilibrium state in presence of a continuous energy source.

Chemists use the following terms interchangeably: far-from-equilibrium, non-equilibrium, off-equilibrium, out-of-equilibrium, away-from-equilibrium, and others. The strict meaning of those terms is that the system is not at a global minimum. However, chemists mostly use those terms such as far-from-equilibrium assemblies to indicate that the systems require a continuous supply of energy to persist. We will uniformly be using "dissipative off-equilibrium" states as their designation.



Renitta Benny is from Kerala (India), and she received her BSc (2016) from Alphonsa College Pala, India and MSc (2018) from St. Thomas College, Pala, India (Mahatma Gandhi University, Kerala). Currently, she is pursuing her PhD under the guidance of Dr Soumen De at the Indian Institute of Science Education and Research (IISER) Thiruvananthapuram, Kerala. Her research interests include switchable metal-organic cages and catalysis.



Diptiprava Sahoo is from Odisha (India), and she obtained her BSc (2017) from Fakir Mohan Autonomous College, Odisha and MSc (2019) from Pondicherry University, Puducherry. During her Master's, she worked with Dr Binoy Krishna Saha on Crystal Engineering. Currently, she is pursuing her PhD under Dr Soumen De at Indian Institute of Science Education and Research (IISER) Thiruvananthapuram. Her research interests include chiral self-sorting and molecular cages.



Ajith George is from Kerala (India). He received his BS-MS degree from the School of Chemistry, Indian Institute of Science Education and Research (IISER) Thiruvananthapuram in 2022. He mainly focussed on the chiral receptor and selective trapping of guest molecules for his major project thesis under the guidance of Dr Soumen De. He likes reading during his spare time.



Soumen De received his MSc (2007) in chemistry from the Indian Institute of Technology Kanpur, India. He earned his PhD degree (2013) from the University of Siegen (Germany) under the guidance of Prof. Michael Schmittl. After completing his first postdoctoral research (2013–2016) with Prof. Ivan Huc at the University of Bordeaux (France), he moved to the Weizmann Institute of Science (Israel) to carry out his second postdoctoral research. Since February 2020, he has held an Assistant Professor position at the Indian Institute of Science Education and Research (IISER) Thiruvananthapuram. His current research interests are out-of-equilibrium operated molecular switches and machines as well as host-guest chemistry.

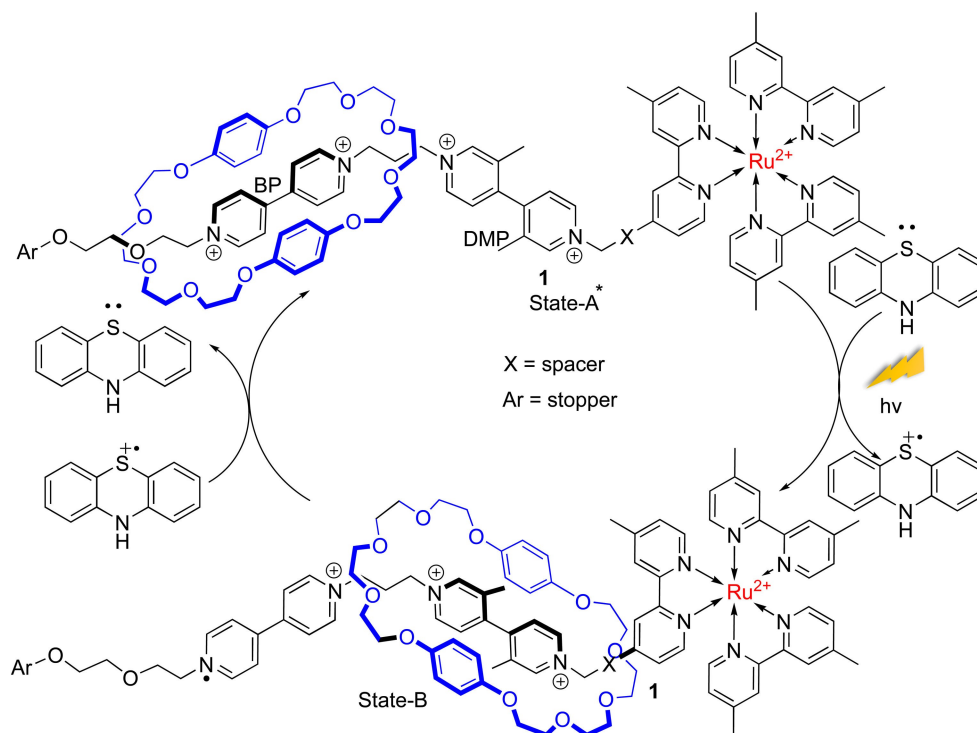
The design principle for a dissipative state is different from an equilibrium one. Generally, an exergonic reaction is coupled with the system to withstand an off-equilibrium state. The following features are essential to successfully construct a fuel-driven autonomous off-equilibrium molecular switch or machine. For simplicity, we will discuss the features for switching between two states. Before adding any stimuli, one of the states should be more stable than another state. After the addition of a stimulus, the system should change its state. This state should be accessible as long as the stimulus is present. The stimulus should undergo auto-decomposition to attain autonomous function. Once the stimulus is consumed, the system should return to its initial state. To access the transient state, the consumption of stimulus should be slow. If unidirectionality is required, additional conditions are essential. There should be a difference in rate between forward and backward motion upon the addition of stimuli. Again, after consuming the stimulus, the forward movement should be faster than the backward motion.

3.1. Light-Powered Molecular Machines

Light is one of the familiar sources of stimuli to control molecular motion. In this context, light is also advantageous over other stimuli as light does not produce any waste and can be used with high spatial and temporal control.^[14] Generally, a light-responsive unit should be attached to the system to fabricate a light-powered autonomous molecular machine. The exact wavelength of light should trigger both switching

methods to induce autonomy. This section will discuss the light-fuelled autonomous operation of off-equilibrium molecular machines.

Stoddart and his group first reported a four-stroke motor's solar-powered autonomous operation based on a rotaxane.^[15] The thread of the rotaxane **1** was composed of two stations: a strongly π -accepting 4,4'-bipyridinium unit (BP) and a weakly π -accepting 3,3'-dimethyl-4,4'-bipyridinium (DMP) unit. Moreover, one end of the thread was functionalised with a tetraaryl-methane group that acted as a stopper. The other terminus was functionalised with $[\text{Ru}(\text{bpy}')_3]^{2+}$ [$\text{bpy}' = 5,5'$ -dimethyl-2,2'-bipyridine] that functioned as a stopper and a photosensitiser. The π -electron-rich bis-*p*-phenylene-34-crown-10 macrocycle was located on the strong π -acceptor BP station in the initial State-A (Scheme 1, State-A). Irradiation of the $[\text{Ru}(\text{bpy}')_3]^{2+}$ complex with 532 nm light in the presence of phenothiazine (ptz) produced a long-lived, strongly reducing excited state that transfers one electron to the BP station. Accordingly, the binding constant between macrocycle and reduced BP decreased. Thus, the macrocycle shuttled from the reduced BP station to the DMP station (Scheme 1, State-B). It is important to note that back electron transfer from the reduced BP unit to $[\text{Ru}(\text{bpy}')_3]^{3+}$ should be slower to observe the ring translocation. Immediately after the transfer of one electron from the excited $^*[\text{Ru}(\text{bpy}')_3]^{2+}$ to the BP unit, $[\text{Ru}(\text{bpy}')_3]^{3+}$ was reduced by ptz via a diffusion-controlled reaction. Therefore, direct reduction of Ru^{3+} via the intramolecular back electron transfer from BP station was prohibited. Hence, ring translocation became the predominant pathway. Finally, electron transfer from the



Scheme 1. The macrocycle's light-powered back and forth motion in a [2]rotaxane. Irradiation of $[\text{Ru}(\text{bpy}')_3]^{2+}$ reduces the BP station via photoinduced electron transfer. Therefore, macrocycle shuttled from the reduced BP station to the DMP station. Back electron transfer to the metal centre oxidises the reduced BP unit, and the macrocycle shuttles back to the BP station. The "*" symbol represents the starting cycle in all the schemes.

reduced BP station to ptz^{+} reinstated the electron-accepting power of the station, and therefore, the macrocycle shifted to its initial state.

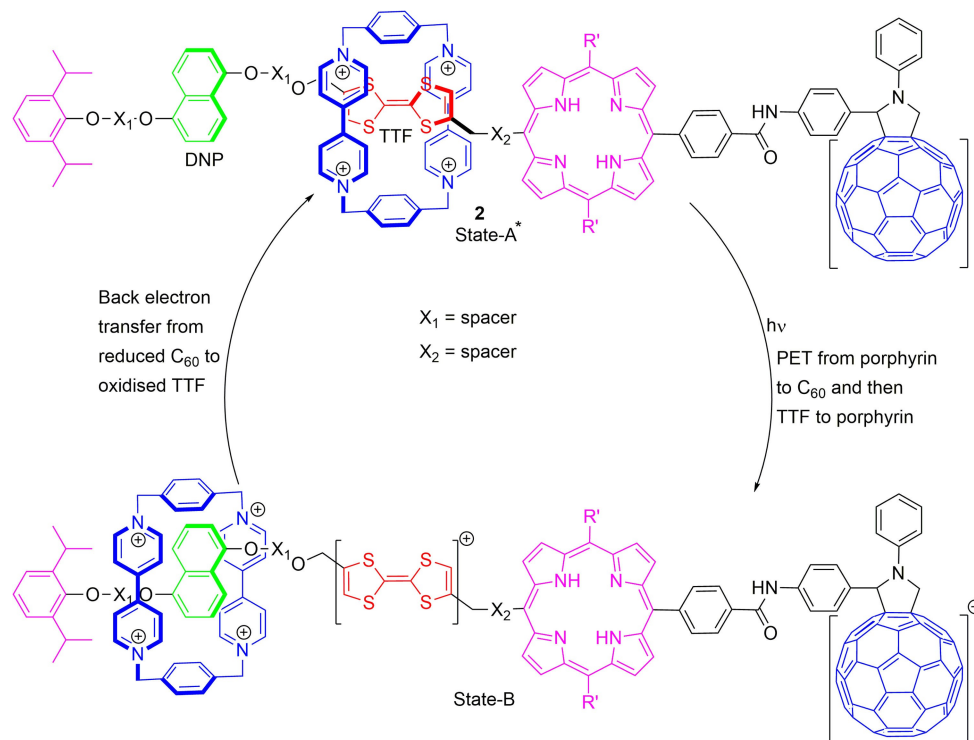
This example illustrates autonomous shuttling of the macrocycle without consuming any chemical fuels. The system also does not produce any waste, and the position of the macrocycle automatically resets to its initial position. It is important to note that under continuous irradiation, the distribution of the macrocycle between two stations would change to a ratio that is different from thermal equilibrium. If the irradiation is stopped, the system will get back to its initial equilibrium state.

Later, a second-generation molecular shuttle was reported by the same group.^[16] Like the 1st generation shuttle, the 2nd generation rotaxane **2** comprised a tetrathiafulvalene (TTF) and a 1,5-dioxynaphthalene (DNP) station. Unlike before, one terminal was equipped with a module for photoinduced charge separation, and the other terminal was functionalised with a diisopropylaromatic unit. Initially, the π -accepting cyclobis(paraquat-*p*-phenylene) (CBPQT⁴⁺) macrocycle resided on the better electron-donor TTF unit (Scheme 2, State-A). The mechanism for the operation of shuttling was similar to before. Thus, the irradiation of porphyrin with visible light triggered an electron transfer from porphyrin to the C₆₀ unit. Subsequent electron transfer from the TTF unit to the oxidised porphyrin unit weakened the initial host-guest complex and the macrocycle shuttled from the TTF station to the DNP station (Scheme 2, State-B). Eventually, the back electron transfers from reduced C₆₀ to oxidised TTF⁺ triggered the translocation of the

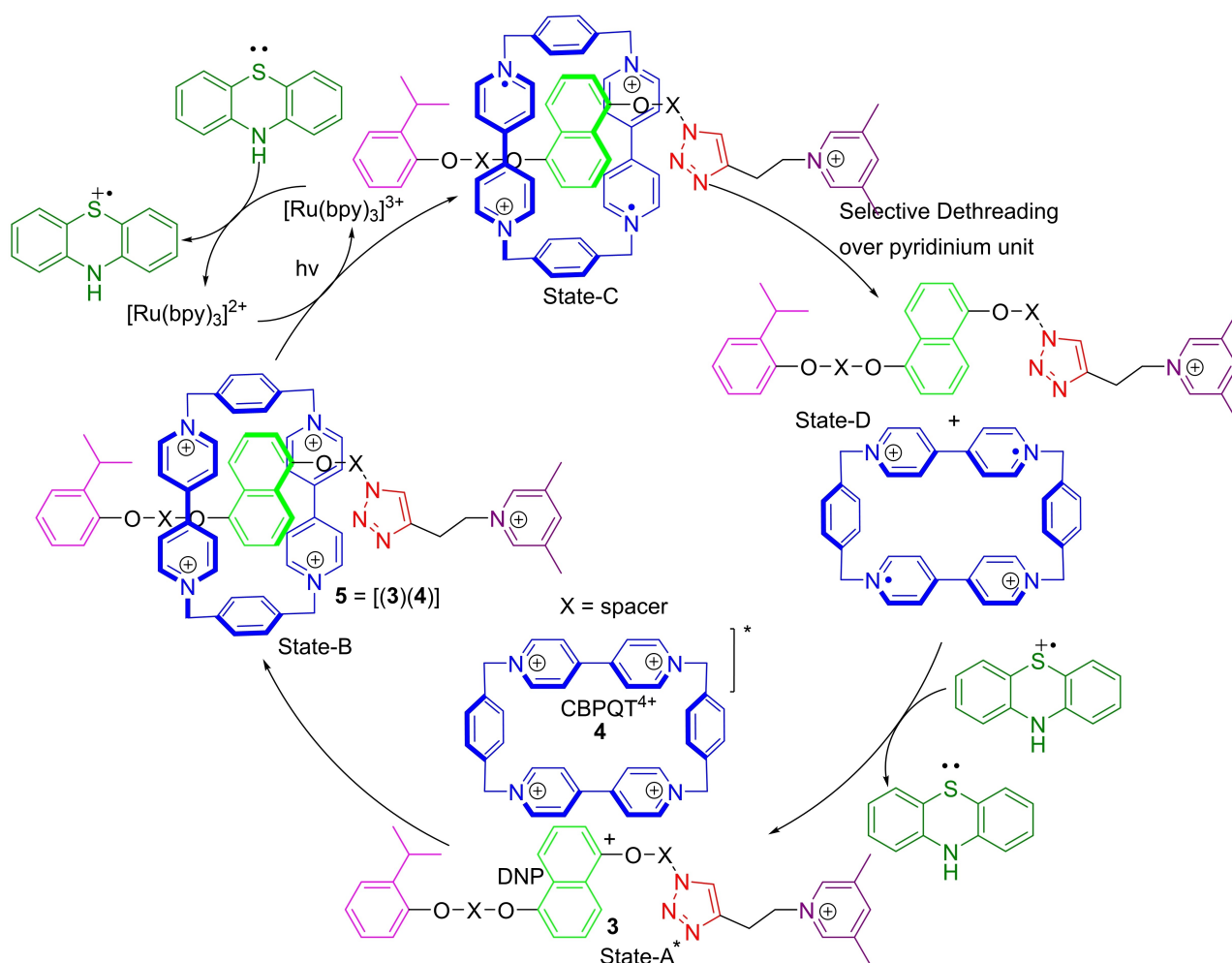
macrocycle from the DNP station to the TTF station to regenerate the initial state.

The same group also reported unidirectional translational movement of the CBPQT⁴⁺ macrocycle along a thread.^[17] The thread contained a π -donating DNP unit in the middle, and the two terminals were functionalised with a positively charged 3,5-dimethylpyridinium unit and a neutral 2-isopropylphenyl group, respectively. Treating the CBPQT⁴⁺ macrocycle with the axle furnished [2]pseudorotaxane **5** through donor-acceptor interactions (Scheme 3, State-B). However, the macrocycle must be threaded on the axle selectively from the bulky neutral 2-isopropylphenyl terminated side (16.9 kcal mol⁻¹) as the other terminal will offer an insurmountable amount of repulsive interaction (22.9 kcal mol⁻¹) between two positively charged species. Subsequent reduction of CBPQT⁴⁺ to CBPQT^{(2+)(•+)} led to the dethreading of the macrocycle due to a decrease in donor-acceptor interactions between the DNP unit and the reduced macrocycle. In contrast to the threading, dethreading selectively occurred over the 3,5-dimethylpyridinium (18.2 vs. 21.3 kcal mol⁻¹) unit due to the substantial decrease in coulombic repulsion providing a minimum energy path. Finally, re-oxidation of CBPQT^{(2+)(•+)} to CBPQT⁴⁺ brought the system back to its original state and prepared it to experience another cycle.

Thus, illuminating the mixture of 2[pseudorotaxane], [Ru(bpy)₃]²⁺ (bpy = 2,2'-bipyridine), and ptz with 450 nm light led to light-triggered electron transfer from the excited state $^*[\text{Ru}(\text{bpy})_3]^{2+}$ to the CBPQT⁴⁺ component of the pseudorotaxane and reduced the macrocycle to the radical cation



Scheme 2. Light-powered back and forth motion of a tetracationic macrocycle in [2]rotaxane. Irradiation of porphyrin triggers electron transfer from porphyrin to the C₆₀ unit. Finally, electron transfer from TTF to oxidised porphyrin leads to the translocation of the macrocycle from the oxidised TTF unit to the DNP unit. Automatic back electron transfer reduces the oxidised TTF, generating initial rotaxane.



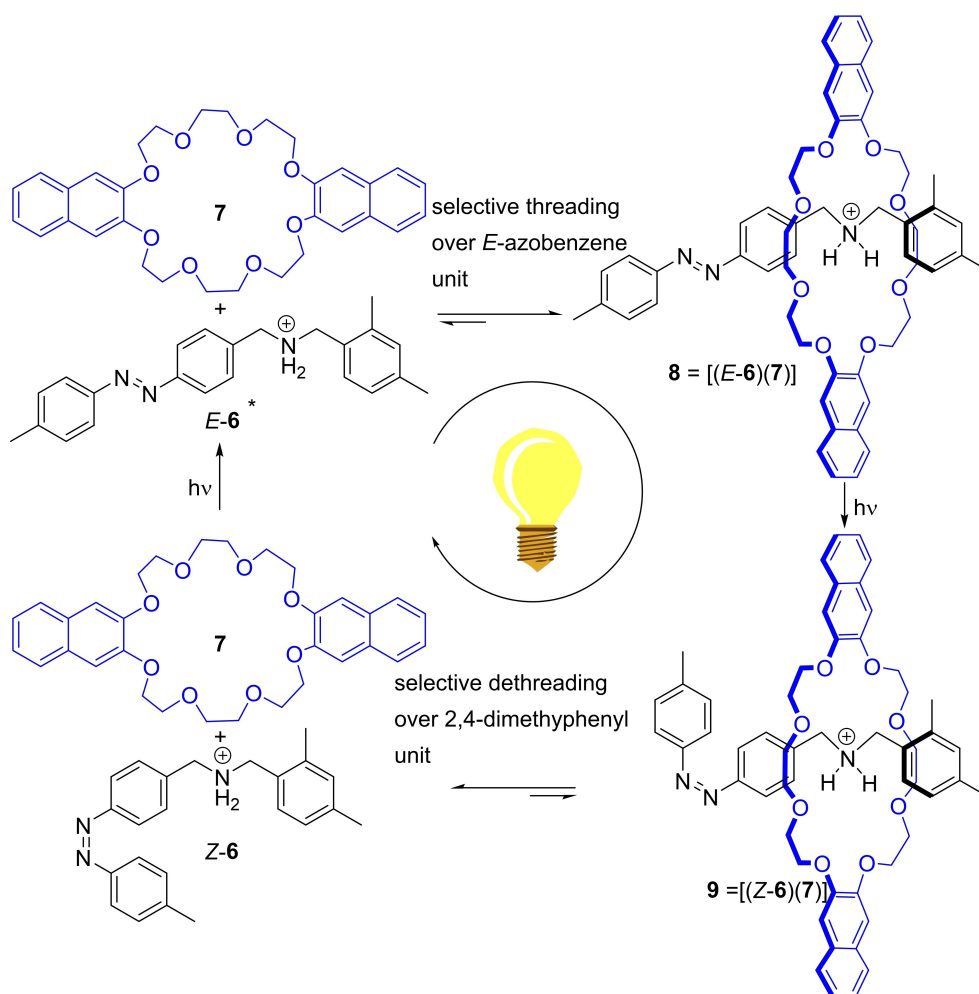
Scheme 3. Light-fuelled relative unidirectional threading-dethreading of CBPQT⁴⁺ macrocycle.

CBPQT^{(2+)(•+)}. The ptz then reacted with [Ru(bpy)₃]³⁺ to regenerate [Ru(bpy)₃]²⁺ and increased the lifetime of the reduced viologens. Hence, dethreading of the macrocycle occurred, but preferentially over the 3,5-dimethylpyridinium end group. Hence, the threading/dethreading of the macrocycle proceeded autonomously with light as the sole stimulus. An off-equilibrium dissipative state could be achieved by reiterating the threading-reduction-dethreading-oxidation cycle under steady irradiation conditions. Unfortunately, the operation of the pump in a dissipative off-equilibrium regime was not validated.

Recently, the same group realised a dual pump^[18] that operated with chemical or electrical fuel. Two pumps were joined in a head-to-tail fashion. The CBPQT⁴⁺ macrocycle entered the axle unidirectionally to form a [2]rotaxane in the first redox cycle but was expelled from the opposite side in the second redox cycle. A unidirectional threading-dethreading motion was accomplished with electrical fuel.

Credi and co-workers also reported an autonomous molecular pump that dissipated light energy to stay away from equilibrium.^[19] Recently, they extended their previous work to a 2nd generation supramolecular pump.^[20] The centre of the thread contained an ammonium group that can act as a station

for 2,3-dinaphtho[24]crown-8-ether macrocycle via hydrogen bonding. One thread terminal was decorated with a pseudo-stopper 2,4-dimethyl phenyl unit, while the other terminal was decorated with a photoswitchable *E*-azobenzene unit. Treating the macrocycle **7** with the axle (*E*-**6**) furnished the pseudorotaxane **8** in which the macrocycle resided on the central ammonium station (Scheme 4). The hydrogen-bonding interactions between the oxygen atoms and the ammonium centre, as well as the π -stacking interactions between naphthalene and planar *trans*-azobenzene units, possibly stabilised ($K=5 \times 10^6 \text{ M}^{-1}$) the pseudorotaxane. It is important to note that the macrocycle entered preferentially over the *E*-azobenzene functionalised terminal ($\approx 82\%$) as the 2,4-dimethyl phenyl unit was bulkier than the *E*-azobenzene. Subsequent irradiation with 365 nm light isomerised the easily threadable *E*-azobenzene into the bulkier unthreadable *Z*-azobenzene ($> 96\%$ in PSS). Simultaneously, the pseudorotaxane ($K=3 \times 10^5 \text{ M}^{-1}$) was also destabilised, possibly due to reduced π -stacking of the naphthalene units of macrocycle with the non-planar *Z*-azobenzene moiety of the thread. As a result, dethreading of the macrocycle occurred. However, the macrocycle cannot be unthreaded via an unsurmountable *Z*-azobenzene terminal. The



Scheme 4. Schematic representation of light-fuelled unidirectional pumping of the macrocycle.

dethreading of the macrocycle must continue preferentially through the bulky 2,4-dimethylphenyl-functionalised terminal (>99%). The initial state can be regenerated again by photochemical or thermal isomerisation of the *Z*- to the *E*-isomer, and thereby the system is set for another round of directional threading. Autonomous light-activated switching between the states under continuous irradiation was achieved as the same light can induce both $E \rightarrow Z$ and $Z \rightarrow E$ isomerisations due to the overlapping absorption spectra of *E*- and *Z*-azobenzene. Accordingly, an off-equilibrium dissipative photostationary state was achieved under continuous irradiation conditions. In this state, the *Z*-enriched complex 9 was present at more than the equilibrium value, although it is thermodynamically less stable than 8.

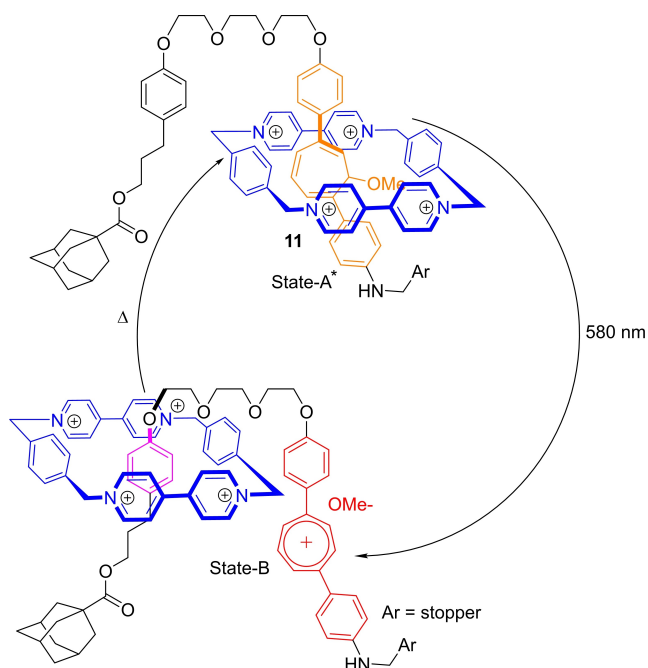
Light has also been used to cleave a covalent bond to generate an off-equilibrium transient state of a rotaxane.^[21] The thread comprised two stations, namely anisole and a diarylcycloheptatriene station. Initially, the CBPQT⁴⁺ macrocycle resided over the diarylcycloheptatriene station (Scheme 5, State-A). Irradiation with 580 nm light generated a tropylium cation. The stability of the inclusion complex decreased, and the macrocycle shifted to the alkoxyphenyl station (Scheme 5,

State-B). The thermal back-reaction reinstated the initial state of the rotaxane. It is important to note that the lifetime of this transient state is 15 s at room temperature. The authors also modified the thread to prepare a light-powered generation of transient states in a linear rotaxane.^[22]

3.2. Acid-Base Reaction-Driven Molecular Switches and Machines

Changing the pH value has been another successful strategy to control switching between two states. To design acid-base reaction-driven autonomous off-equilibrium molecular switches and machines, the addition of acid should induce a forward switching process. The deprotonated acid should undergo decarboxylation to yield a much stronger base that can abstract the released proton. The system would then reset to its initial state.

Di Stefano and his co-workers first reported an acid as fuel to induce the reversible switching between two states of a catenane. The [2]catenane 13 comprised two identical interlocked macrocyclic alkenes bearing 1,10-phenanthroline units



Scheme 5. Light triggered autonomously back and forth motion of a [2]rotaxane 11. Initially, the macrocycle resided over the diarylcycloheptatriene station. Illumination with 580 nm light generated a tropylium cation, and the macrocycle translocated over the alkoxyphenyl unit. Automatic recapturing of the tropylium ion by methoxide regenerated diarylcycloheptatriene and the macrocycle shuttled to its initial position.

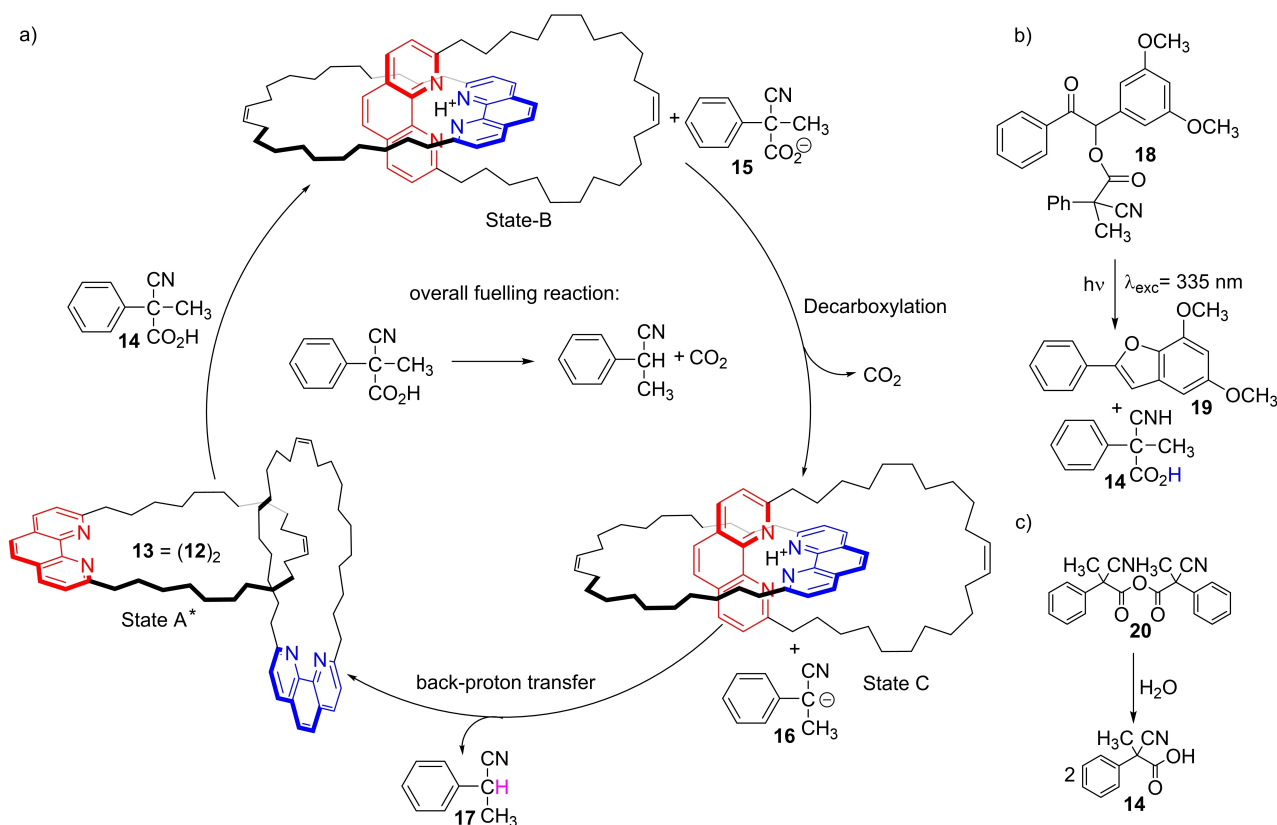
(12) in their backbone.^[23] In the absence of an acid, the catenane existed in State-A without any well-defined co-conformation of the two macrocycles (Scheme 6). The addition of one equivalent of 2-cyano-2-phenylpropanoic acid (CPA, 14) triggered the protonation of one of the phenanthrolines to form a Sauvage-type catenane. Thus, the macrocycle underwent a large-amplitude motion from the neutral State-A to a well-defined protonated State-B. The concurrently generated carboxylate anion 15 slowly decarboxylated and formed the much stronger base 16 that abstracted the proton from the protonated catenane. Overall, adding one equivalent of acid changed the catenane from State-A to State-B to State-C to State-A, and the system was ready for another fuelling cycle. It was important to note that when catenane 13 (2 mM) was treated with acid 14 (4 mM) in DCM, excess acid was consumed within 8 min of addition, as evidenced by ¹H NMR spectroscopy. The system returned to its initial state within one hour to start the second fuelling cycle.

In another example, the authors demonstrated that the fuel could be generated in situ by irradiating a pre-fuel, 18, with 335 nm light.^[24] This irradiation produced controlled amounts of acid 14 and 19 (Scheme 6b). The same cyclic motion between co-conformation of catenane was realised by irradiating a mixture of catenane 13 and pre-fuel 18. In another example, the author combined acid decarboxylation with a chemical reaction rather than a photochemical reaction. The switching between different co-conformations of catenane 13 could be repeatedly initiated for several iterative cycles through the

nonstop release of acid 14 by hydrolysing the corresponding anhydride 20 in the presence of a small amount of water.^[25] The authors also reported that the release rate of fuel from the pre-fuel can be controlled chemically.^[26]

The same group utilised 14 and its derivatives as fuel to trigger switching between two states of the bistable [2]rotaxane 21 (Scheme 7).^[27] The thread of the rotaxane comprised a dialkylammonium (NH_2^+) and a BP unit that serve as recognition sites for the nitroxide-functionalised macrocycle. Initially, the macrocycle resided on the ammonium station by hydrogen bonding. However, addition of diisopropylethylamine (iPr_2EtN) deprotonated the ammonium unit, leading to the shuttling of the macrocycle from the former ammonium station to the BP station. Further addition of TFA regenerated the initial state. After establishing the acid-base shuttling, the author used 14 as fuel to switch between two stations. In this case, the starting point was a deprotonated State-A where the macrocycle complexed around the BP unit (Scheme 7, State-A). Adding one equivalent of 14 protonated the amine group as expected. The macrocycle shifted to the ammonium station (State-B) within a few seconds, as evidenced by EPR spectroscopy. The carboxylate anion 15 automatically underwent decarboxylation and generated a strong base 16 that deprotonated the ammonium station. Accordingly, the macrocycle shifted to its initial BP station over 60 min. The system became ready for the second round of fuel. The author demonstrated three iterative cycles of refuelling. It is important to note that the back proton transfer was faster when a *para*-chloro-substituent was used, and it then took approximately 20 min to complete an entire cycle. However, back proton transfer did not occur with *para*-methyl or *para*-methoxy substituents due to competing side reactions, and the backward switching process failed. The same group also reported dissipative operation of a DNA-based nanodevice using 14 as fuel.^[28]

The use of CPA as fuel was taken up by Schmittl and co-workers demonstrating a series of fuel-driven operations of molecular switches. The first example in the series was the fuel-driven oscillating emission of a [2]rotaxane 22 (Scheme 8).^[29] The rotaxane axle comprised two degenerate triazolium stations linked via a short dibenzylammonium (DBA) bridge. Both axle ends were functionalised with anthracene units as stoppers and fluorescent probes. Initially, the benzo crown (DB24 C8) macrocycle selectively resided on the central DBA station through hydrogen bonding (Scheme 8, State-A). However, the addition of DBU triggered the deprotonation of the DBA station. Subsequently, the macrocycle shuttled from the DBA station to the triazolium station. After a successful demonstration of shuttling of the DB24 C8 macrocycle by successive addition of acid and base, the authors explored the use of 14 as a fuel to control the state of the rotaxane. Adding one equivalent 14 to the State-A of rotaxane 22 led to the protonation of the central amine unit. Accordingly, the DB24 C8 macrocycle shuttled from the triazolium station to the DBA station in a ratio of 1:3 (State-B). The generated carboxylate anion 15 released carbon dioxide to form the stronger base 16 that deprotonated the DBA station. Therefore, the binding affinity of the DB24C8 macrocycle was reversed, and the macrocycle shuttled from the DBA



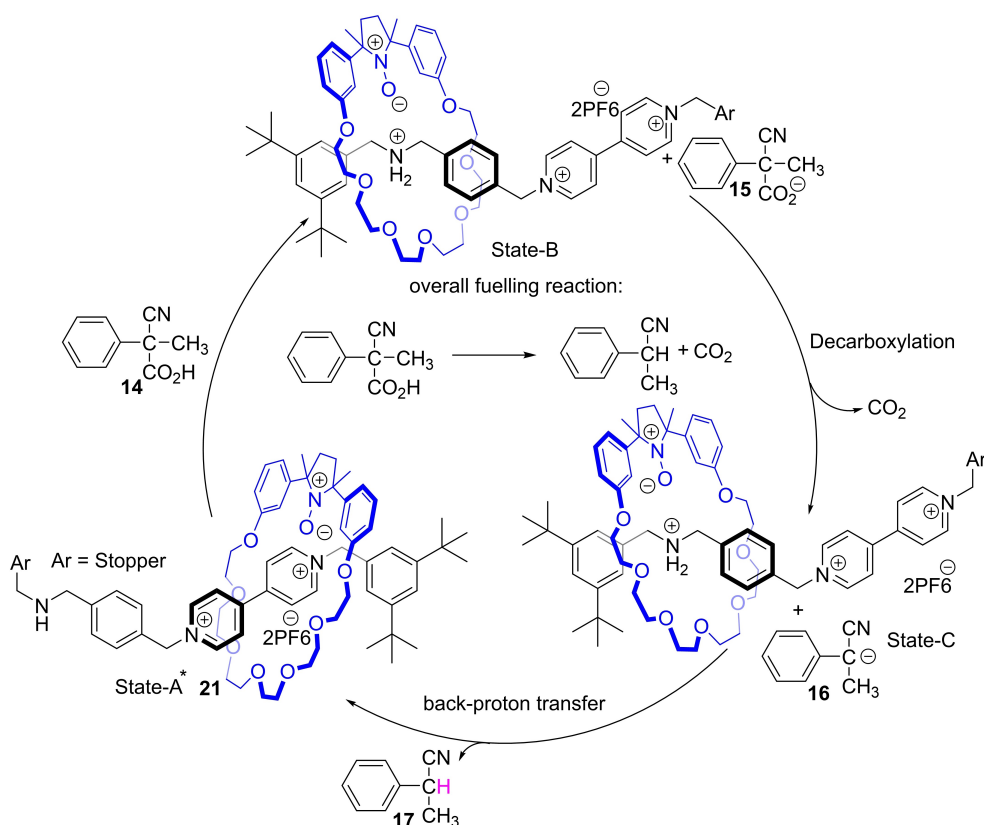
Scheme 6. The schematic representation of (a) CPA-fuelled switching between [2]catenane states. (B) the generation of CPA fuel from photolysis of pre-fuel **18**; (c) hydrolysis of pre-fuel **20** (CPA = 2-cyano-2-phenylpropanoic acid, **14**).

station to the triazolium station, leading to the regeneration of the initial rotaxane after 9 min. NMR and fluorescence emission intensity supported the fuel-driven shuttling process. As the triazolium units were blocked by the macrocycle in the initial state, PET from excited anthracene to triazolium unit was prevented, and anthracene showed fluorescence emission. In contrast, the rotaxane did not exhibit any fluorescence emission in State-B because of the quenching of fluorescence via PET from the excited anthracene to the triazolium units.

In another report, Schmittel et al. utilised the same acid **14** as a fuel to control off-equilibrium signal transduction among various switches.^[30] Mixing hexacyclen (**23**), nanoswitch **24**, luminophore **25**, Zn^{2+} ions, and Li^+ ions in an appropriate ratio yielded NetState A (Scheme 9). In this state, Zn^{2+} bound to **23** ($\log K = 17.8$),^[31] whereas Li^+ bound to nanoswitch **24** instead of **25**. The supply of one equivalent of TFA protonated the complex $[\text{Zn}(\text{23})]^{2+}$, leading to the release of Zn^{2+} that replaced Li^+ from nanoswitch $[\text{Li}(\text{24})]^+$. Finally, the discharged Li^+ formed a complex with **25** ($\log K = 4.36$), producing NetState-B composed of $[(\text{23})(\text{H})]^+$, $[(\text{24})\text{Zn}]^{2+}$, and $[(\text{25})\text{Li}]^+$. This switching was supported by ^1H NMR spectroscopy and a shifting of the fluorescence emission maximum from $\lambda = 554$ to 512 nm due to the formation of $[(\text{25})\text{Li}]^+$. However, the supply of DBU took out the proton from $[(\text{23})(\text{H})]^+$, which triggered cascaded backward reactions (shifting of Zn^{2+} from $[(\text{24})\text{Zn}]^{2+}$ to **23** and Li^+ from $[(\text{25})\text{Li}]^+$ to **2** to generate the NetState-A. After successfully demonstrating acid-base switching between two states, the

authors used **14** as a fuel. The supply of one equivalent **14** to the NetState-A immediately generated the NetState-B, as evidenced by the immediate shifting of the fluorescence intensity maximum from 554 to 512 nm. Deprotonated acid **15** then underwent decarboxylation, producing the strong base **16**. Subsequently, $[(\text{23})(\text{H})]^+$ experienced deprotonation, thereby leading to the regeneration of NetState-B. The regeneration was completed within 42 min as supported by the shifting fluorescence intensity maximum from 512 to 554 nm. Reversible switching between two states was performed with fuel **14** for four cycles.

The Schmittel group^[32] also demonstrated the CPA-fuelled dissipative synthesis of the pseudorotaxane rotor **29** (Scheme 10). The rotor was realised based on the clean self-sorting in the presence of ligands **23**, **26**, **27**, **28**, Zn^{2+} and protons. In NetState-II, Zn^{2+} was coordinated by the phenanthroline unit of ligand **28** and the terpyridine unit of ligand **27**. The pyridine unit coordinated to the zinc porphyrin station, and the crown ether moiety of ligand **27** formed a complex with the protonated amine of ligand **26**. The Netstate-II was comprised of $[(\text{23})(\text{H})]^+$ and rotor **29**. The exchange frequency in rotor **29** was found to be 15.4 kHz at 298 K. After realising the five-component rotor, the authors also demonstrated the formation and operation of the rotor away from equilibrium. Thus, NetState-I was achieved when ligands **23**, **26**, **27**, **28** and Zn^{2+} were mixed in a 1:1:1:1:1 ratio. In this state, Zn^{2+} was coordinated with ligand **23**, leaving all other ligands unaffected.



Scheme 7. The schematic representation of CPA-fueled back and forth motions of paramagnetic rotaxane **21**. The addition of **14** to State-A led to the protonation of amine. The macrocycle shifted from BP to ammonium station to yield State-B. Decarboxylation of acetate followed by the capture of the proton from the ammonium station restores the initial State-A.

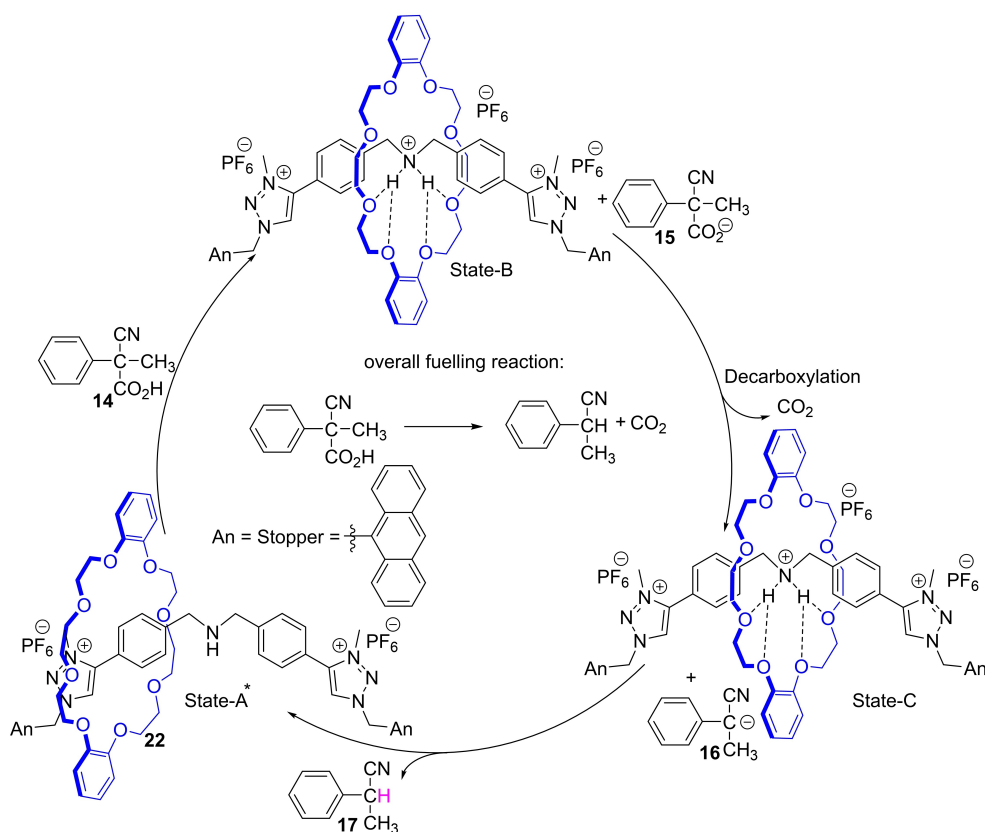
The addition of **14** (2 equiv.) protonated $[Zn(23)]^{2+}$, thereby liberating Zn^{2+} that combined with ligands **27** and **28** in a HETTAP fashion. Another equivalent of acid protonated the amine of ligand **26**. Finally, the combination of both these complexes delivered NetState-II composed of $[(23)(H)]^+$ and rotor **29** = $[Zn(26-H^+)(27)(28)]^{2+}$. Again, after decarboxylation of the acid, the so-generated strong base recovered the protons, commanding the disassembly of rotor **29**. The fuel-driven switching between both states was reported for up to five cycles.

In a recent example, Schmittl et al.^[33] showed the utilisation of two different fuels, **14** and Ag^+ , in stimulating multistage speed oscillations of a turnstile. Turnstile **30** is comprised of two shielded phenanthroline units that acted as the stator and a terpyridine arm that functioned as a rotor (Scheme 11). In the presence of two equivalents of stimulus (Ag^+ , Li^+ , H^+), molecular turnstile **30** transformed into a metal rotor, as evidenced by 1H NMR spectroscopy and ESI-MS. It was found that the rotational frequency of the proton rotor, silver rotor, and lithium rotor at 298 K amounted to 84.0 kHz, 1.57 Hz and 0.38 Hz, respectively. The rotor was also assembled under dissipative off-equilibrium conditions. Adding two equivalents of **14** protonated the two phenanthroline stations of turnstile **30**. The formation of the rotor was evidenced by the decrease of fluorescence intensity of the turnstile at $\lambda = 400$ nm. However, the decarboxylation of the carboxylate anion followed by

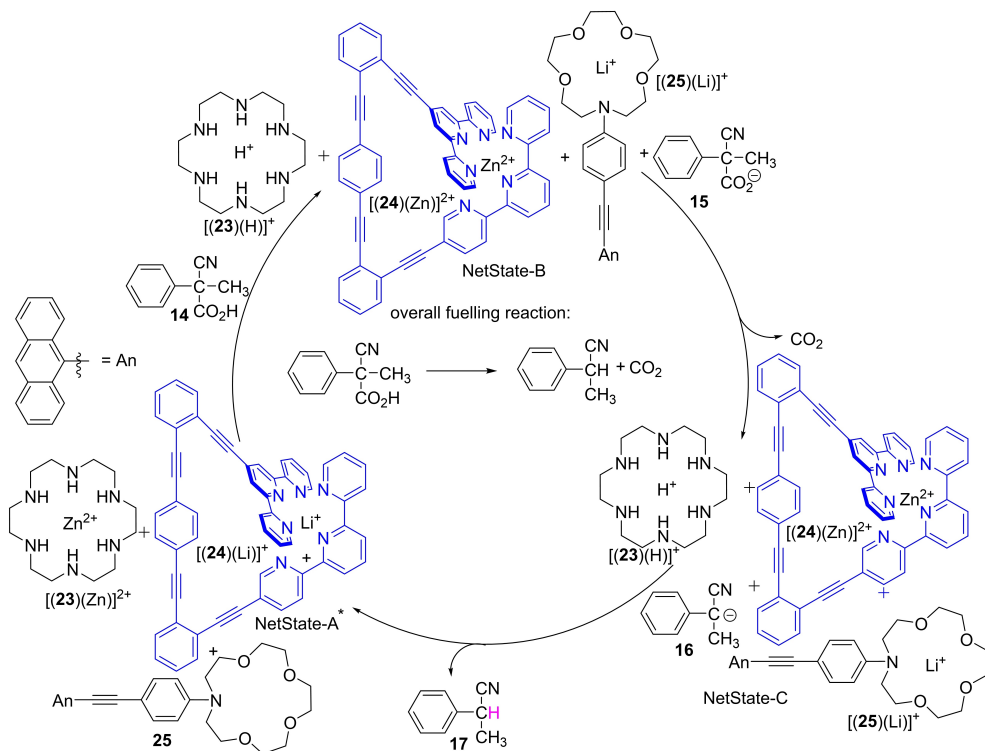
the capture of the proton by a stronger base regenerated the turnstile **30**. The fluorescence intensity was thus recovered within 135 min of adding CPA. After establishing the CPA as fuel to form the rotor, the authors also demonstrated the Ag^+ as fuel to set up the same rotor. Thus, adding Ag^+ in the presence of **31** and **32** to the turnstile **30** generates $[(30)Ag_2]^{2+}$. With time, **31** and **32** reacted to form **33**, and a bromide ion left as a leaving group. The released bromide ion then captured the Ag^+ from the rotor leading to the regeneration of the initial turnstile. In the process, the rotor changed its oscillation speed form (fast = **(30)** → slow = $[Ag_2(30)]^{2+}$ → stop = $[Ag(30)]^+$ → fast = **(30)**). Depending on the reactants, it was possible to regulate the lifetime of the silver(I) ions in the rotor sites and the period of the oscillating cycle. Very recently, Schmittl and co-workers also reported on the dissipative formation of a device from a cage in the presence of **14** as fuel.^[34]

Decarboxylative fuels are not restricted to only CPA and its derivatives. Fundamentally, all those carboxylic acids which undergo decarboxylation after deprotonation can be used as fuel. The rate of decarboxylation determines the lifetime of the transient species.

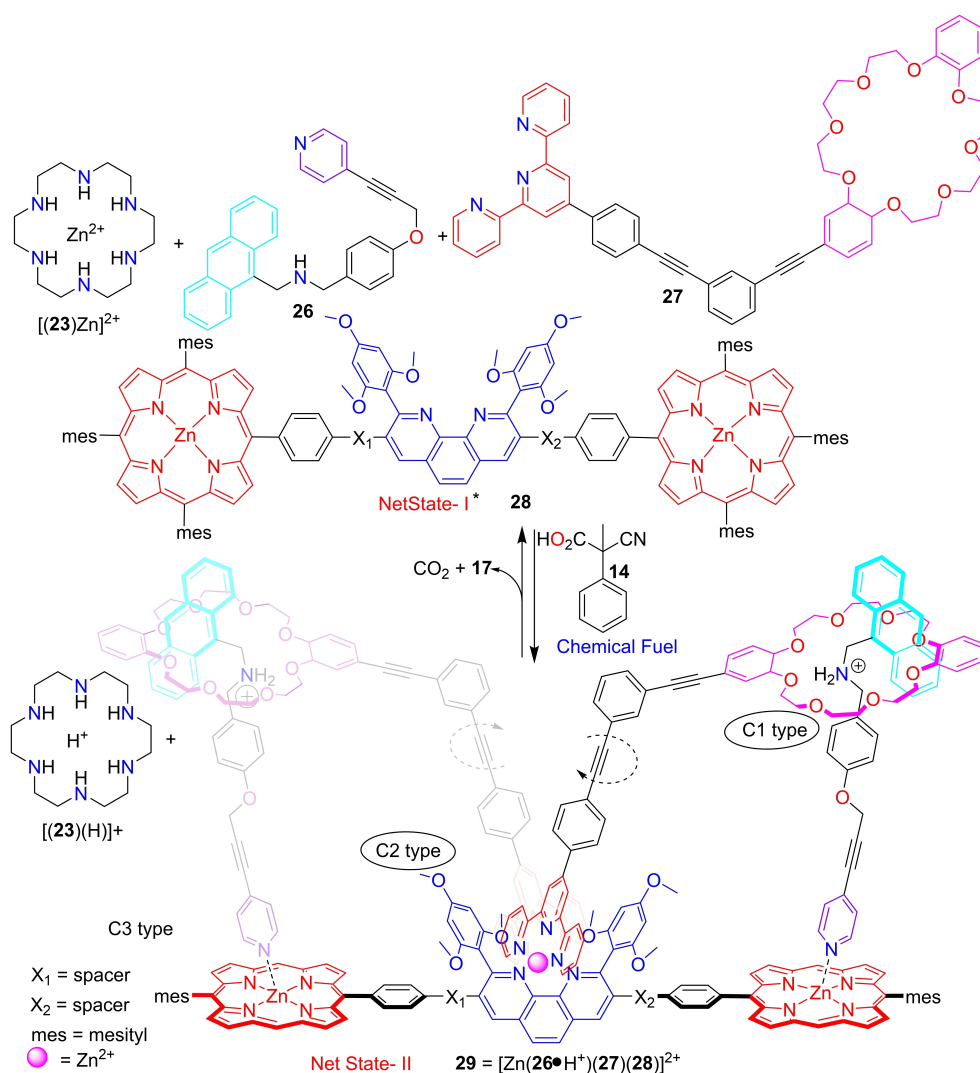
In 2017, David Leigh and co-workers^[35] developed trichloroacetic acid (TCA) as fuel to drive synthetic rotary and linear molecular motors. The system took advantage of altering the relative association constant of macrocycles for different binding stations on circular or linear tracks. The thread was also



Scheme 8. The schematic representation of CPA-fuelled back and forth motions of rotaxane 22. The addition of 14 to State-A led to the protonation of the amine. The macrocycle shifted from the triazolium station to the ammonium station to yield State-B. Slow decarboxylation of 15 followed by the capture of the proton from the DBA station restored the initial State-A.



Scheme 9. Schematic representation of CPA-fuelled cascaded communication.



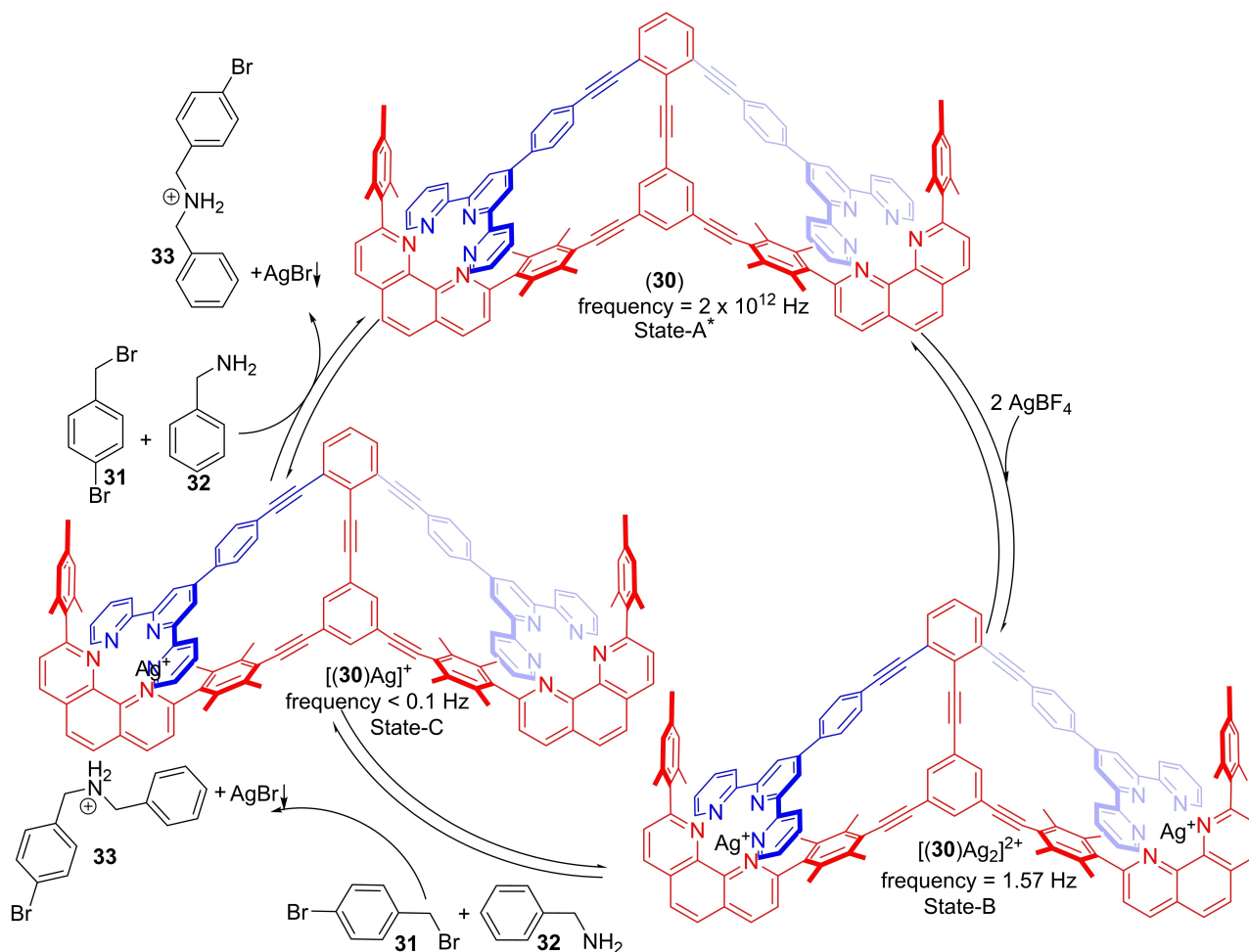
Scheme 10. Schematic representation of CPA-fuelled dissipative formation of transient pseudorotaxane **29**. Net state-1 was fabricated by mixing one equivalent of ligand **23**, **26**, **27**, **28** and Zn²⁺. Upon adding **14**, ligand **23** gets protonated, inducing metal translocation from [Zn(**23**)]²⁺ to **28** and transiently producing **29**. **29** again disintegrated over time to its individual components by auto-decarboxylation of carboxylic acid, followed by recapturing the proton from [H(**23**)]⁺.

equipped with bulky hydrazones and disulfide barriers that can be removed in acidic and basic conditions.

Due to weak electrostatic attraction, the macrocycle encircled the triazolium station in the neutral state (Scheme 12, State-A). Upon adding a 4:1 mixture of TCA and triethylamine, the binding affinity towards the macrocycle got reversed due to the protonation of the dibenzyl amine unit of the track. The macrocycle can reach the DBA station over hydrazone or the disulfide barrier. Under these acidic conditions, the macrocycle, however, cannot be transported over disulfide as the disulfide is kinetically stable. In contrast, as the hydrazone group exchanges (kinetically labile) in acidic conditions, it produces a short-lived aldehyde (Scheme 12, State-B) that cannot block the movement of the macrocycle. Thus, 90% of the macrocycle shifted to the DBA station in a clockwise direction over short-lived aldehyde after 15 h. During the acid-induced translocation of the crown-ether, trichloroacetic acid was decomposed to CO₂

and CHCl₃ by triethylamine. After 17 h, the system transformed to basic pH by decomposing all of the TCA and removing all the protons from the DBA station. As a result, the binding affinity of the macrocycle again reversed. At the same time, the hydrazone unit became kinetically locked in the basic condition, and the disulfide started to undergo exchange with the solution. Consequently, the crown-ether shifted clockwise to the original triazolium station over the transient thiol (Scheme 12, State-D, generated during disulfide exchange). Therefore, a single pulse of the chemical fuel triggered an autonomous full 360° clockwise revolution of 87% of the macrocycle. The same group also demonstrated the fuel-driven operation of a molecular pump based on the same mechanism.

Recently, David Leigh and his co-workers reported an application of a fuel-driven switching between two stations of a rotaxane.^[36] Due to the higher binding affinity of the thiourea group towards the DB24 C8 macrocycle (log *K* = 3.70), it was



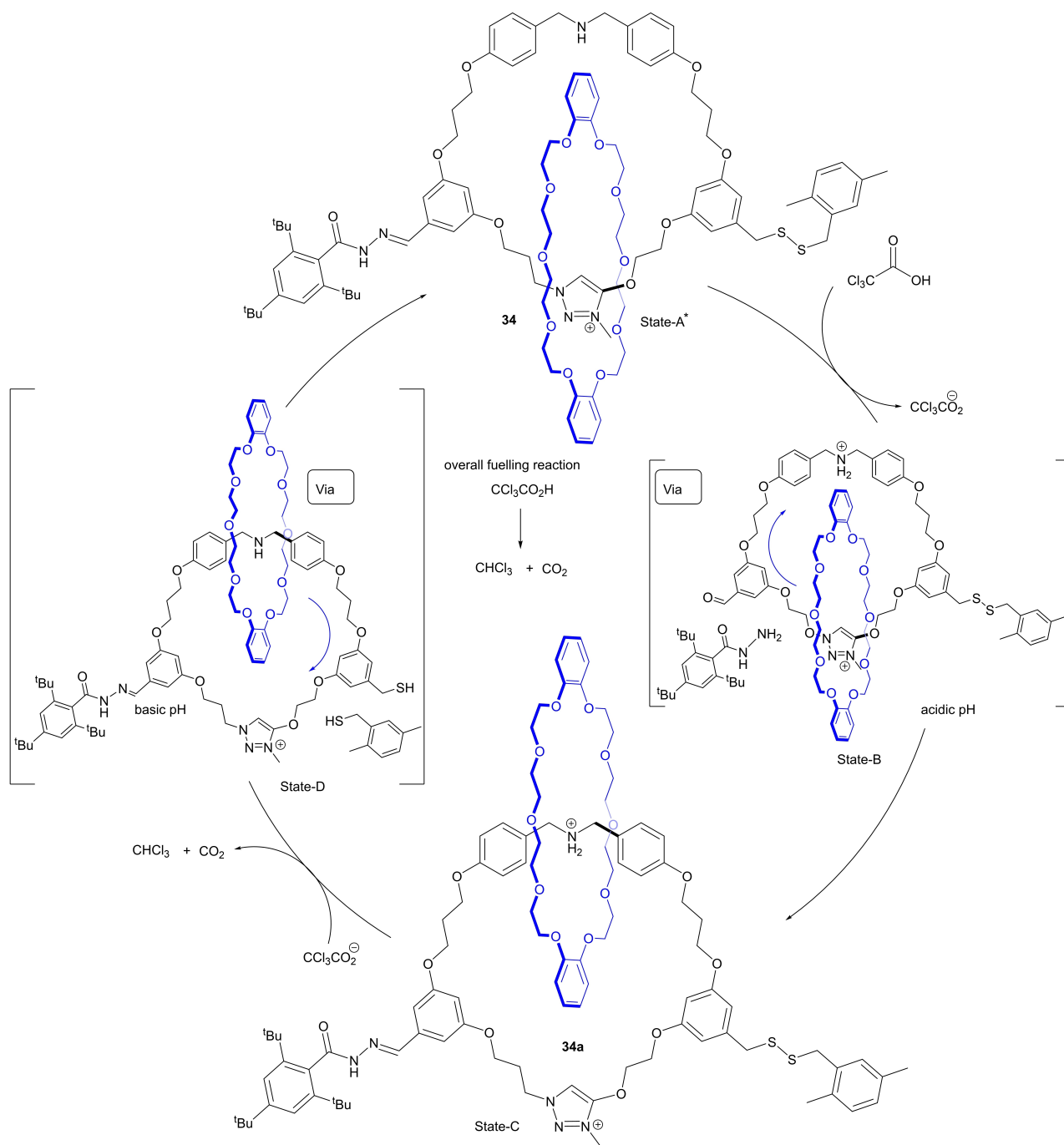
Scheme 11. The schematic representation of off-equilibrium speed control of the rotor fuelled by Ag^+ ions. The addition of 2 equiv. AgBF_4 to the turnstile 30 furnished a rotor with a frequency of 1.57 Hz. In situ present 31 and 32 reacted together in an $\text{S}_{\text{N}}2$ fashion releasing a bromide ion, precipitating out one equivalent of Ag^+ as AgBr . Thus, a new rotor was formed with a frequency < 0.1 Hz. A second 2^{nd} $\text{S}_{\text{N}}2$ reaction precipitated the other silver ion to regenerate the initial rotor.

initially located on the thiourea station instead of the amine station (Scheme 13, State-A). However, adding TCA to the rotaxane protonated the amine group, reversing the binding affinity. As a result, the DB24C8 macrocycle shuttled from the thiourea station to the ammonium station (Scheme 13, State-B). This transient state persevered over approximately 9 h until the decarboxylation of excess acid had finished. After this time, the decarboxylation of the trichloroacetate anion started to produce the strongly basic trichloromethane anion that reclaimed the proton from the ammonium station. Consequently, over 7 h, the DB24C8 macrocycle was fully translocated from the ammonium station to the thiourea station. Up to seven iterative fuelling cycles were performed to validate the robustness of the dissipative cycling. Moreover, as the thiourea moiety was available in the transient State-B and State-C, hydrogenation of nitrostyrene was possible (ON). After regeneration of the initial state, the catalysis rate was decreased. It was important to note that the lifetime of the transient state can be controlled by fluctuating the quantity of fuel supplied. The

above example demonstrated the first example of a dissipative catalyst based on a molecular machine.

3.3. Protection–Deprotection-Triggered molecular machines

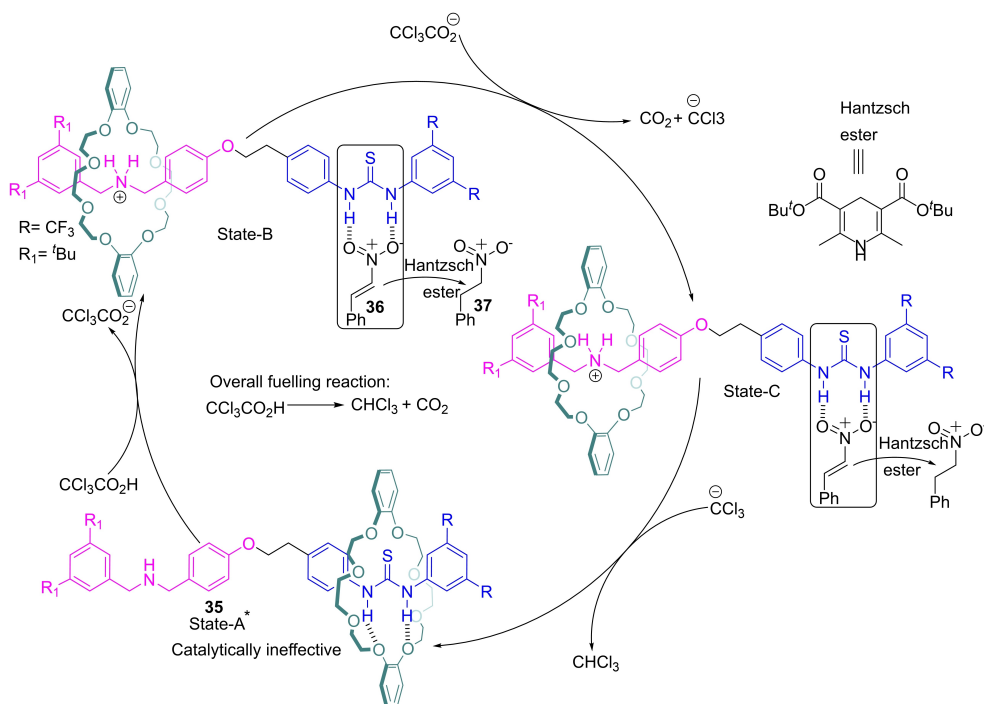
Besides acid-base reaction-driven off-equilibrium molecular switches, protection-deprotection chemistry has also been utilised to achieve the off-equilibrium states of molecular switches. In this approach, one functional group is protected with an appropriate protecting group that will deprotect autonomously under the reaction conditions to generate the initial state. The system will sustain its off-equilibrium conditions as long as the protecting group reagent (fuel) is present in the system. Once the reagent is consumed, the system will return to equilibrium. In this respect, David Leigh and co-workers^[37] have designed and synthesised 9-fluorenylmethoxycarbonyl chloride, Fmoc-Cl-fuelled autonomous small-molecule motors that run without further interference. The motor was based on the [2]catenane 38, where two different macro-



Scheme 12. TCA-fuelled unidirectional rotation of the macrocycle along the track.

cycles were intertwined (Scheme 14). The larger size macrocycle served as the track for the smaller macrocycle. The two fumaramide units acted as a station for the benzylic amide units of the smaller macrocycle. Directly after each fumaramide station, a removable carbonate unit blocked the movement of the small ring to go forward. However, after removing the carbonate group, the ring can proceed further. It was found that the cleavage of the carbonate was independent of the macrocycle's position. However, the carbonate formation was faster when the macrocycle was further away as the macrocycle

prevented nucleophilic attack by the hydroxyl group on a large electrophile. Thus, the treatment of catenane FumD₂-39 with Fmoc-Cl in the presence of a catalyst (R)-41 yielded preferentially FumD₂-38 rather than FumH₂-38 (20:80 FumH₂-38:FumD₂-38). Similarly, the reaction of catenane FumH₂-39 should selectively produce FumH₂-38 rather than FumD₂-38. However, removing both the Fmoc groups of 38 generated FumH₂-39 or FumD₂-39 in equal proportion. Consequently, the Fmoc group tended to follow the macrocycle on the path, confirming that forward movement was always faster than the reverse. Con-



Scheme 13. Schematic representation of the operation of the dissipative catalyst **35**. In the neutral state, the macrocycle encircled over the thiourea unit via hydrogen bonding, and therefore, this state is catalytically ineffective (State-A). Upon addition of pulses of TCA, the amine unit was protonated. Therefore, the macrocycle shifted from the thiourea station to the ammonium station leading to the demasking of the thiourea unit. Then, the thiourea moiety was effective in catalysing the reduction of β -nitrostyrene. Decarboxylation of trichloroacetate, followed by recapturing the protons from the ammonium station, regenerated the initial rotaxane.

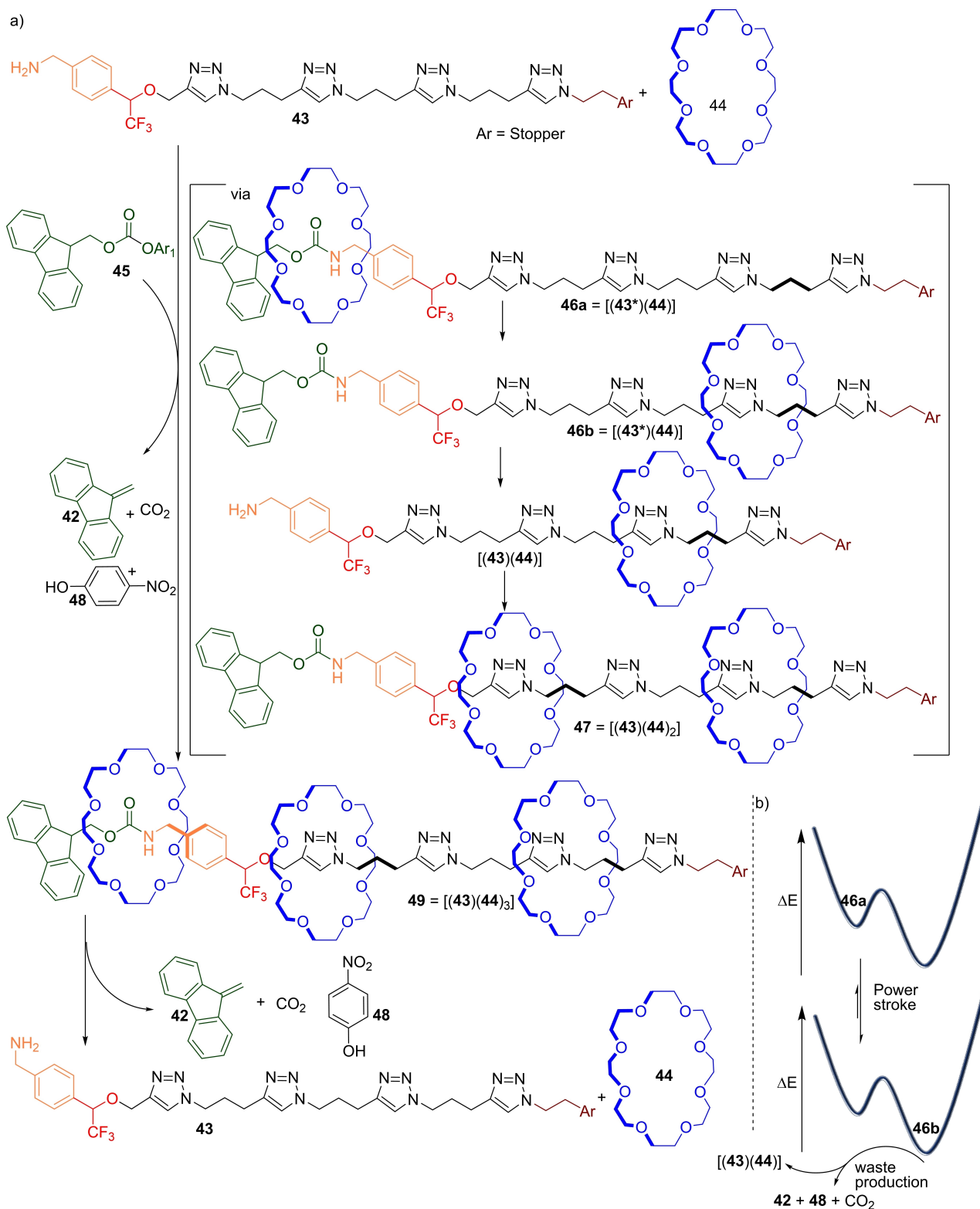
sequently, the small ring continuously travelled directionally along the path like a train by diffusing between two static fumaramide stations as long as the chemical fuel, Fmoc-Cl, was present in the system. It was shown that both the Fmoc attachment and the cleavage reaction to and from the catenane occurred under motor-operating conditions. The efficiency of the process would be at a maximum when sufficient amounts of Fmoc-Cl were present for the protection reaction to proceed rapidly as soon as a hydroxyl group was exposed. The build-up of the catenane diol can be avoided and will prevent the small ring from being free to shuttle around the track without directional bias. It is important to note that the macrocycle's net-directional movement speed was around 12 h for each 360° rotation.

Likewise, Fmoc-carbonate has also been used as fuel to drive an autonomous molecular pump based on a rotaxane (Scheme 15).^[38] The body of axle **43** comprised a chain of triazole heterocycles connected by short alkyl spacers. In contrast, the N-terminus of the axle contained a benzylamine, and the other terminal was decorated with a bulky triarylme-thine stopper. Due to the weak interaction between the triazole units and crown ethers, the equilibrium percentage of crown ethers relocated from bulk solution onto the triazole station was very small. The benzylamine of the axle got Fmoc-protected in the presence of Fmoc-carbonate, 24-crown-8 and diisopropylamine (DIPEA). This reaction was catalysed by the cavity of the crown ether and acted as a template to form

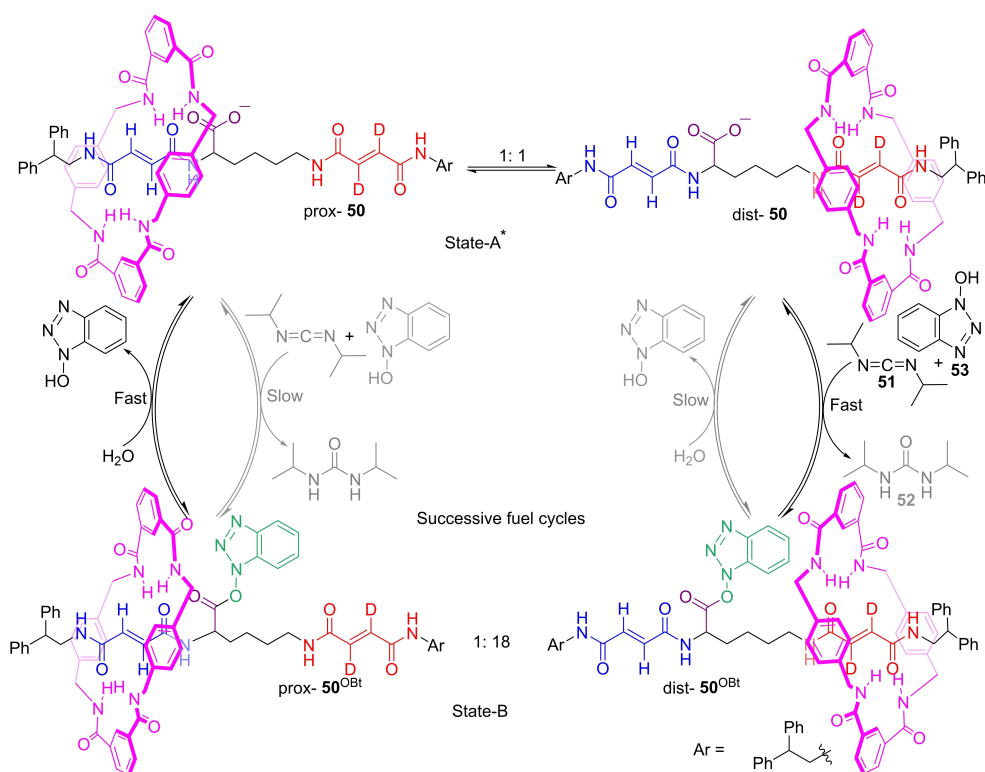
[2]rotaxane, where the macrocycle was located on the carbamate station through hydrogen bonding.

The thus generated Fmoc-carbamate group inhibited the dethreading of the ring into the solution. The trifluoromethyl substituent near the benzylamine moiety is of the appropriate size to allow slow slippage of the crown ether ring to the axle. Over time, the crown ether ring slowly moved to the triazole units as the triazole groups should form more favourable interactions with the crown ether than the sterically encumbered benzylic carbamate unit. The presence of DIPEA triggered the decomposition of Fmoc-carbamate to dibenzofulvene and CO_2 to generate the amine for further pumping cycles. In this way, the crown ethers were arrested from the bulk solution to the restricted section of the axle and sustained in an off-equilibrium state as long as the chemical fuel was present in the solution. The system returned to its initial equilibrium when the fuel was finished. It is important to note that the formation of [2]rotaxane was much faster than the dethreading of the macrocycle. The N-terminus of [(**43**)(**44**)] underwent further active template formation to pump a second (and third) ring onto the axle before breaking down to the individual components.

Besides Fmoc derivatives, carbodiimide has also been used as fuel to switch the macrocycle's position in a rotaxane from an equilibrium state to an off-equilibrium state.^[39] The thread of the rotaxane **50** contained two fumaramide stations and a carboxylate group to block or unblock the passage of the macrocycle. Initially, the macrocycle was distributed between



Scheme 15. (a) Schematic representation of Fmoc-carbonate-fuelled dissipative capture of the macrocycle onto the thread. The addition of thread and the macrocycle in the presence of Fmoc-carbonate trapped the macrocycle onto the thread. The carbamate protection was hydrolysed under the reaction conditions to produce the free amine. It reacted with another molecule of Fmoc-carbonate to trap another macrocycle molecule onto the ring. In this way, multiple macrocycles were captured onto the thread as long as fuel was present. When the fuel was used up, the [n]rotaxane disintegrated into individual components. In the typical reaction conditions, the pump (1 equiv.) was mixed with the macrocycle (10 equiv.) and Hünig's base (15 equiv.). The fuel was continuously added over 16 h via syringe pump as a solution in toluene (0.2 M) at a 0.7 equiv./h rate. (b) Energy hypersurface of the pump fuelling cycle.



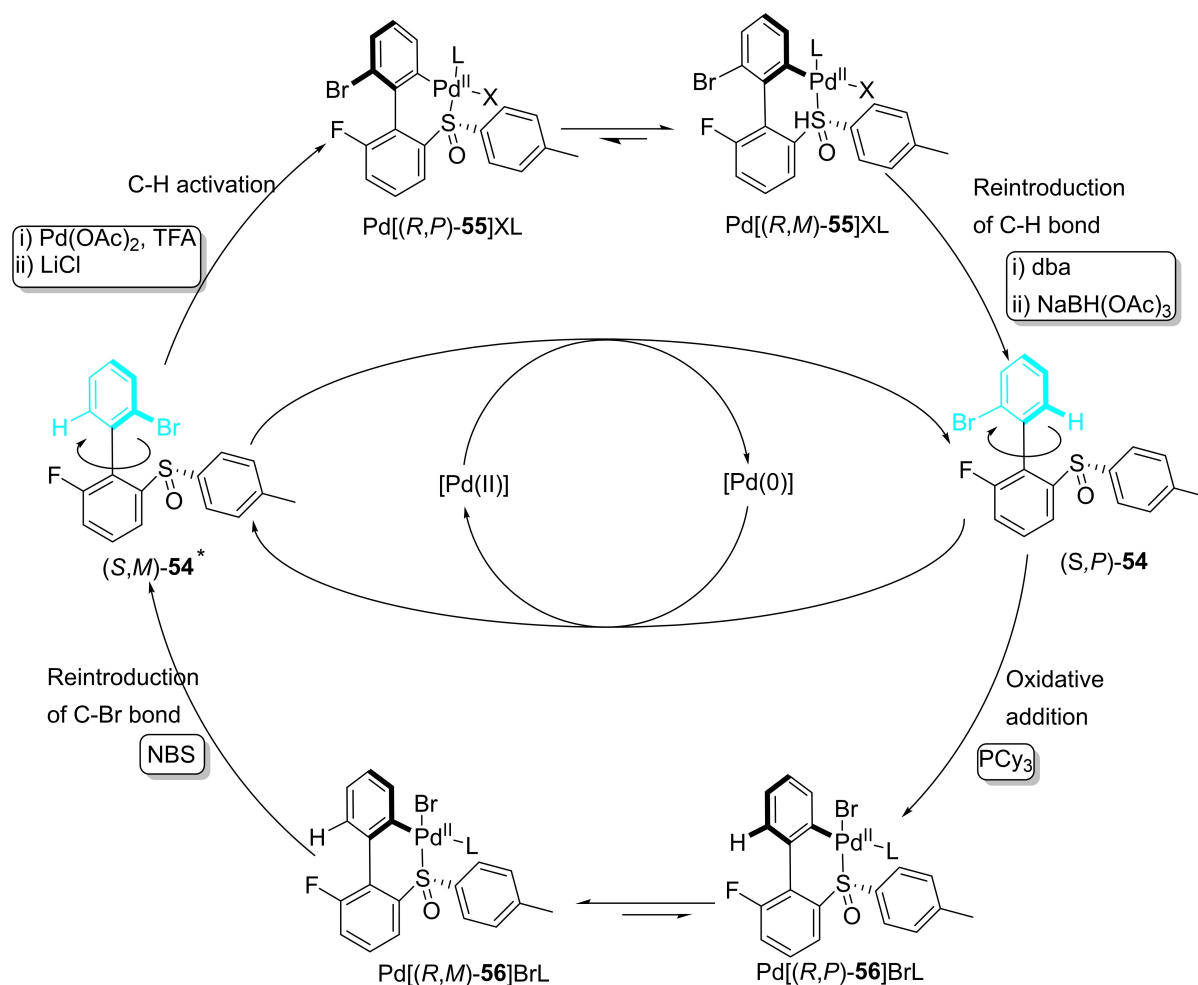
Scheme 16. Schematic representation of the dissipative formation of triazole ester barrier to macrocycle translocation. The rotaxane dist-50 reacted faster with carbodiimide fuel to form triazole ester, followed by rapid replacement by the OBT barrier. The active ester was hydrolysed under the reaction conditions producing initial rotaxane. However, the hydrolysis rate of prox-50^{OBT} was faster than dist-50^{OBT}. Therefore, every cycle increased the ratio of dist-50^{OBT} to prox-50^{OBT}, reaching up to 1:18.

3.4. Oxidation-Reduction-Induced Molecular Machines

Besides acid–base reactions and protection-deprotection chemistry, oxidation-reduction reactions have also been used as fuel to control molecular switches and machines. In this regard, Feringa and co-workers^[41] reported the fuel-driven autonomous operation of a synthetic molecular motor based on the fundamental reactivity differences of metal in different oxidation states. The motor takes advantage of biaryl **54**, which can exist as two atropisomers, (*S,M*)-**54** and (*S,P*)-**54**. The first chiral descriptor (*S*) arises due to static point chirality at sulfur; *M* and *P* represent the dynamic chirality that arises due to the stereogenic axis. The molecules were configurationally stable due to the high energy barrier for rotation around a carbon-carbon single bond. However, forming a linkage between the *ortho* substituents of the top and bottom aryl units may significantly reduce the energy barrier to atropisomerisation. The reaction of diastereomerically pure (*S,M*)-**54** with palladium acetate in the presence of TFA and LiCl led to the formatting of a six-membered palladacycle as shown in Scheme 17 and the barrier to atropisomerisation was significantly diminished. Moreover, it was found by DFT calculations that Pd[(*R,M*)-**55**]XL was lower in energy than the diastereomeric Pd[(*R,P*)-**55**]XL by 15.0 kJ mol⁻¹, thereby shifting the equilibrium to Pd[(*R,M*)-**55**]XL. Treatment of this mixture with sodium triacetoxyborohydride led to the formation of (*S,P*)-**54** over (*S,M*)-**54** (>98%) and palladium(0) species. Overall, one aryl group completed a

unidirectional clockwise 180° rotation through a sequence of C–H activation, ligand exchange, hydride transfer, followed by reductive elimination. Rather than purifying the mixture, if tricyclohexylphosphine was added and the temperature was increased, a slight increase in oxidative addition occurred with the in-situ-generated Pd(0) and a new palladacycle Pd[(*R,P*)-**56**]BrL was formed. Consequently, due to the reduction of the energy barrier to atropisomerisation, palladacycle Pd[(*R,P*)-**56**]BrL interconverted to Pd[(*R,M*)-**56**]BrL on account of better stability. Treatment of this mixture with *N*-bromosuccinimide generated a mixture of (*S,M*)-**54** and (*S,P*)-**54** with a ratio of 1:1.32. Overall, a unidirectional 360° revolution of one aryl group over the other around a single bond was achieved, driven by sodium triacetoxyborohydride and *N*-bromosuccinimide as chemical fuels.

In another example, Shi and co-workers reported switching between the two stations of [2]-rotaxane **57** using iodosobenzene as fuel. The axle of the rotaxane comprised a pyridine unit and a C₆ alkyl chain.^[42] The helicene-based macrocycle preferentially encapsulated the C₆ alkyl chain in a neutral state (Scheme 18, State-B). However, the addition of TFA protonated the pyridine unit of the axle. Consequently, the macrocycle shuttled from the alkyl chain to the pyridinium station (Scheme 18, State-A). Again the system went back to its initial state upon treatment with iodosobenzene (PhIO) that traps the TFA as [bis(trifluoroacetoxy)iodo]benzene (BTAIB). After establishing the TFA-triggered shuttling of the macrocycle, shuttling

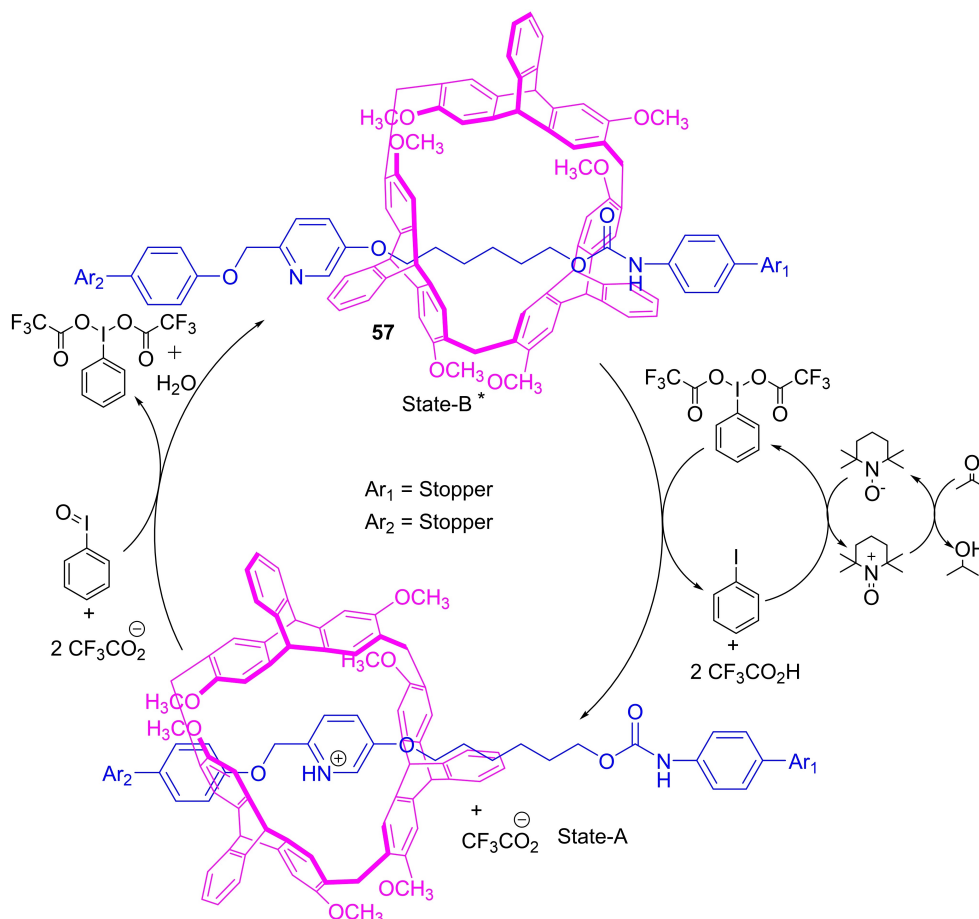


Scheme 17. The schematic representation of unidirectional 360° rotation of a molecular motor powered by a palladium redox cycle. 180° clockwise rotation of the upper ring (from $(S,M)\text{-}54$ to $(S,P)\text{-}54$) was effected by a three-step protocol. Treatment of $(S,M)\text{-}54$ with $\text{Pd}(\text{OAc})_2$ and TFA followed by ligand exchange with LiCl produced the palladacycle. Re-introduction of the C–H bond by reacting the palladacycle with *dba*, followed by sodium triacetoxyborohydride, afforded $(S,P)\text{-}54$ and $\text{Pd}(0)$. Again, the addition of PCy_3 to the reaction mixture initiated oxidative addition to form another palladacycle. Treatment of this palladacycle with NBS regenerated the initial state. Overall, the upper ring rotates 360° in clockwise fashion.

was performed using iodosobenzene as a fuel. To make the process fuel-driven, the authors coupled two reactions: i) reaction of PhIO with TFA to produce BTAIB and ii) in the presence of BTAIB, TEMPO can oxidise isopropanol to acetone with concomitant release of TFA. Thus, the addition of PhIO to rotaxane $(57)(\text{H})^+$ induced TFA consumption, leading to the translocation of the macrocycle over the C_6 alkyl chain. The successive oxidation of *i*-PrOH to acetone in the presence of BTAIB regenerated TFA. The released TFA protonated the pyridine unit of the axle, and the macrocycle shuttled to the pyridinium station. It is important to note that TFA consumption in the presence of PhIO was faster than TEMPO-mediated release of TFA. Thus, the system stayed in State-B as long as PhIO was present. Once the PhIO was entirely consumed, the system automatically returned to the initial state. The authors reported four fuelling cycles.

4. Conclusions

The examples presented in this review indicate an enormous interest in fuel-driven off-equilibrium molecular switches and machines. The review also addresses the critical issues of designing off-equilibrium molecular switches and machines and their peculiar energetic and structural features. Most of the approaches to drive the systems away from equilibrium comprise two or more opposite reactions (e.g., protonation and deprotonation) under the same reaction conditions. Nevertheless, identifying those reactions is not always easy. Kinetic parameters play a central role in dissipative far-from-equilibrium molecular switches and machines. The deactivation step should be slower than the activation step to detect the steady-state concentrations of the far-from-equilibrium state. There should be kinetic asymmetry between several reactions to obtain a directional motion.^[43] The system can function either stepwise or autonomously depending on whether the energy is supplied batch-wise or continuously. Dissipative states can be realised



Scheme 18. Schematic representation of PhIO-fuelled back and forth motion in a [2]catenane.

and detected when the energy is constantly supplied, and an autonomous manoeuvre is required to attain a D State.

Although the synthetic machines discussed in this review are significantly less sophisticated and orders of magnitude smaller than their biological counterparts, they accomplish a fundamental task similar to natural machines. These examples validate the proof of principle by autonomous operation under off-equilibrium conditions using a suitable fuel. It is important to note that the reported off-equilibrium states in most cases do not possess a special function or property. Therefore, more examples of dissipative molecular switches and machines having some functions are anticipated. For example, David Leigh and co-workers have shown that the far-from-equilibrated state of molecular switches could be used in controlling catalytic activity.

Unquestionably, the research on the fuel-driven autonomous operation of molecular machines is highly arduous due to the complexity of coupling an energy dissipation process to a molecular machine. Identifying both the activation and deactivation reactions operating under identical reaction conditions is challenging. Although chemists have many chemical reactions at their disposal, the number of fueling reactions to operate the switches and machines away from equilibrium is yet small. Therefore, the discovery of many more fuels is expected. The

build-up of waste at the end of every cycle decreases the efficiency of the switching process. Hence, using those fueling reactions that yield only gas waste or precipitate the waste from the solution would be more advantageous. Otherwise, light as fuel is an attractive option as it does not produce any waste; reusing the waste to fuel by some other catalytic reactions is also another viable option. Another problem is the functional group compatibility of the machines in the presence of fuels and their competing background decomposition.

Nevertheless, fuel-driven off-equilibrium operated molecular switches and machines have the following advantages: (i) they mimic biological counterparts (ii) they display autonomous behaviour like motor proteins; (iii) they do not produce/produce less waste products depending on the stimuli, and (iv) their two-way operation only needs one stimulus. Indeed, tremendous prospects lie in fabricating fuel-driven off-equilibrium molecular switches and machines with different properties from the equilibrium version. Undoubtedly the field of artificial fuel-driven off-equilibrium molecular machines is still in its infancy, but with the increasing number of groups involved in this hot topic, substantial progress and achievements are anticipated to be realised in the near future.

Acknowledgements

S. D. gratefully acknowledges the financial assistance from IISER Thiruvananthapuram and SERB, DST, India (SRG/2020/001486). R. B wishes to acknowledge DST/INSPIRE/03/2019/001025 (IF190401) for her fellowship. D. S and A. G. acknowledge the support from IISER Thiruvananthapuram.

Conflict of Interest

The authors declare no conflict of interest.

Data Availability Statement

Data sharing is not applicable to this article as no new data were created or analyzed in this study.

Keywords: dissipative · fuel · machines · molecular switches · off-equilibrium

- [1] I. Aprahamian, *ACS Cent. Sci.* **2020**, *6*, 347–358.
- [2] M. Baroncini, S. Silvi, A. Credi, *Chem. Rev.* **2020**, *120*, 200–268.
- [3] a) S. A. P. van Rossum, M. Tena-Solsona, J. H. van Esch, R. Eelkema, J. Boekhoven, *Chem. Soc. Rev.* **2017**, *46*, 5519–5535; b) S. De, R. Klajn, *Adv. Mater.* **2018**, *30*, 1706750.
- [4] S. Amano, S. Borsley, Z. Sun, D. A. Leigh, *Nat. Nanotechnol.* **2021**, *16*, 1057–1067.
- [5] Y. Feng, M. O'valle, J. S. W. Seale, C. K. Lee, D. J. Kim, R. D. Astumian, J. F. Stoddart, *J. Am. Chem. Soc.* **2021**, *143*, 5569–5591.
- [6] C. J. Bruns, J. F. Stoddart, *Acc. Chem. Res.* **2014**, *47*, 2186–2199.
- [7] M. V. Delius, D. A. Leigh, *Chem. Soc. Rev.* **2011**, *40*, 3656–3676.
- [8] V. Blanco, D. A. Leigh, V. Marcosi, *Chem. Soc. Rev.* **2015**, *44*, 5341–5370.
- [9] A. Goswami, S. Saha, P. K. Biswas, M. Schmittel, *Chem. Rev.* **2020**, *120*, 125–199.
- [10] C. Pezzato, C. Cheng, J. F. Stoddart, R. D. Astumian, *Chem. Soc. Rev.* **2017**, *46*, 5491–5507.
- [11] K. Kinbara, T. Aida, *Chem. Rev.* **2005**, *105*, 1377–1400.
- [12] C. Biagini, S. D. Stefano, *Angew. Chem. Int. Ed.* **2020**, *59*, 8344–8354; *Angew. Chem.* **2020**, *132*, 8420–8430.
- [13] E. R. Lay, D. A. Leigh, F. Zerbetto, *Angew. Chem. Int. Ed.* **2007**, *46*, 72–191; *Angew. Chem.* **2007**, *119*, 72–196.
- [14] D. Sahoo, R. Benny, N. Kumar, K. S. S. De, *ChemPlusChem* **2022**, *87*, e202100322.
- [15] V. Balzani, M. Clemente-León, A. Credi, B. Ferrer, M. Venturi, A. H. Flood, J. F. Stoddart, *PNAS* **2006**, *103*, 1178–1183.
- [16] S. Saha, A. H. Flood, J. F. Stoddart, S. Impellizzeri, S. Silvi, M. Venturi, A. Credi, *J. Am. Chem. Soc.* **2007**, *129*, 12159–12171.
- [17] H. Li, C. Cheng, P. R. McGonigal, A. C. Fahrenbach, M. Frascioni, W. G. Liu, Z. Zhu, Y. Zhao, C. Ke, J. Lei, R. M. Young, S. M. Dyar, D. T. Co, Y. W. Yang, Y. Y. Botros, W. A. Goddard, M. R. Wasielewski, R. D. Astumian, J. F. Stoddart, *J. Am. Chem. Soc.* **2013**, *135*, 18609–18620.
- [18] Y. Qiu, L. Zhang, C. Pezzato, Y. Feng, W. Li, M. T. Nguyen, C. Cheng, D. Shen, Q. H. Guo, Y. Shi, K. Cai, F. M. Alsaibia, R. D. Astumian, J. F. Stoddart, *J. Am. Chem. Soc.* **2019**, *141*, 17472–17476.
- [19] G. Ragazzon, M. Baroncini, S. Silvi, M. Venturi, A. Credi, *Nat. Nanotechnol.* **2015**, *10*, 70–75.
- [20] M. Canton, J. Groppi, L. Casimiro, S. Corra, M. Baroncini, S. Silvi, A. Credi, *J. Am. Chem. Soc.* **2021**, *143*, 10890–10894.
- [21] W. Abraham, L. Grubert, U. W. Grummt, K. Buck, *Chem. Eur. J.* **2004**, *10*, 3562–3568.
- [22] S. Schmidt-Schäffer, L. Grubert, U. W. Grummt, K. Buck, W. Abraham, *Eur. J. Org. Chem.* **2006**, 378–398.
- [23] J. A. Berrocal, C. Biagini, L. Mandolini, S. D. Stefano, *Angew. Chem. Int. Ed.* **2016**, *55*, 6997–7001; *Angew. Chem.* **2016**, *128*, 7111–7115.
- [24] C. Biagini, F. D. Pietri, L. Mandolini, O. Lanzalunga, S. D. Stefano, *Chem. Eur. J.* **2018**, *24*, 10122–10127.
- [25] C. Biagini, G. Capocasa, V. Cataldi, D. D. Giudice, L. Mandolini, S. D. Stefano, *Chem. Eur. J.* **2019**, *25*, 15205–15211.
- [26] C. Biagini, G. Capocasa, D. D. Giudice, V. Cataldi, L. Mandolini, S. D. Stefano, *Org. Biomol. Chem.* **2020**, *18*, 3867–3873.
- [27] P. Franchi, C. Poderi, E. Mezzina, C. Biagini, S. D. Stefano, M. Lucarini, *J. Org. Chem.* **2019**, *84*, 9364–9368.
- [28] D. Mariottini, D. D. Giudice, G. Ercolani, S. D. Stefano, F. Ricci, *Chem. Sci.* **2021**, *12*, 11735–11739.
- [29] A. Ghosh, I. Paul, M. Adlung, C. Wickleder, M. Schmittel, *Org. Lett.* **2018**, *20*, 1046–1049.
- [30] A. Ghosh, I. Paul, M. Schmittel, *J. Am. Chem. Soc.* **2019**, *141*, 18954–18957.
- [31] P. R. Varadwaj, A. Varadwaj, G. H. Peslherbe, H. Marques, *J. Phys. Chem. A.* **2011**, *115*, 13180–13190.
- [32] A. Ghosh, I. Paul, M. Schmittel, *J. Am. Chem. Soc.* **2021**, *143*, 5319–5323.
- [33] A. Goswami, S. Saha, E. Elramadi, A. Ghosh, M. Schmittel, *J. Am. Chem. Soc.* **2021**, *143*, 14926–14935.
- [34] D. Mondal, A. Ghosh, I. Paul, M. Schmittel, *Org. Lett.* **2022**, *24*, 69–73.
- [35] S. Earbas-Cakmak, S. D. P. Fielden, U. Karaca, D. A. Leigh, C. T. McTernan, D. J. Tetlow, M. R. Wilson, *Science* **2017**, *358*, 340–343.
- [36] C. Biagini, S. D. P. Fielden, D. A. Leigh, F. Schaufelberger, S. D. Stefano, D. Thomas, *Angew. Chem. Int. Ed.* **2019**, *58*, 9876–9880; *Angew. Chem.* **2019**, *131*, 9981–9985.
- [37] M. R. Wilson, J. Solà, A. Carlone, S. M. Goldup, N. Lebrasseur, D. A. Leigh, *Nature* **2016**, *534*, 235–240.
- [38] S. Amano, S. D. P. Fielden, D. A. Leigh, *Nature* **2021**, *594*, 529–534.
- [39] S. Borsley, D. A. Leigh, B. M. W. Roberts, *J. Am. Chem. Soc.* **2021**, *143*, 4414–4420.
- [40] S. P. Fletcher, F. Dumur, M. M. Pollard, B. L. Feringa, *Science* **2005**, *310*, 80–82.
- [41] B. S. L. Collins, J. C. M. Kistemaker, E. Otten, B. L. Feringa, *Nat. Chem.* **2016**, *8*, 860–866.
- [42] Q. Shi, C. F. Chen, *Chem. Sci.* **2019**, *10*, 2529–2533.
- [43] R. D. Astumian, *Nat. Commun.* **2019**, *10*, 3837–3850.

Manuscript received: June 3, 2022

Revised manuscript received: August 16, 2022